Offshore transport of organic carbon by upwelling filaments in the Canary Current System

Santana-Falcón, Yeray[a,b], Mason, Evan[c,d], Arístegui, Javier[b]

[a] *Université Grenoble Alpes, CNRS, IRD, Grenoble INP, IGE, (Grenoble), France*
[b] *Instituto de Oceanografía y Cambio Global, IOCAG, Universidad de Las Palmas de Gran Canaria, ULPGC, Las Palmas de Gran Canaria, Las Palmas, Spain*
[c] *Applied Physics Laboratory, University of Washington, Seattle, Washington*
[d] *Mediterranean Institute for Advanced Studies (IMEDEA), Esporles, Mallorca, Spain*

Abstract

A coupled physical-biogeochemical model (ROMS-PISCES) forced by climatological fields is used to examine the role of upwelling filaments in the offshore exchange of particulate (POC) and dissolved (DOC) organic carbon in the Canary Current eastern boundary upwelling system (CanC EBUS). In this region, mesoscale filaments at Capes Ghir (∼30.5 °N) and Juby (∼27.5 °N) have been frequently described using both observational and numerical data. Due to their semi-permanent presence and unique dynamical characteristics, studies focusing on filaments often provide an incomplete picture of the physical and biological processes at work, and their effects on coast-to-ocean export. The present model experiment confirms the complex three-dimensional structure of the filaments that comprises both offshore and onshore flow components. The model shows strong seasonal variability in the offshore transport mediated by the filaments. Recirculation at the edges of the filaments returns water towards the shore, especially in autumn when they are diverted northwards by the large scale boundary circulation. By contrast, offshore transport peaks during late spring - early summer when onshore recirculation is limited. Overall, the estimated net annual offshore flux of excess total organic carbon (e-TOC, the non-refractory pools of DOC and POC) averages 2.0 $\times$ 10^9 kg C y^{-1}, and may increase up to 4.3 $\times$ 10^9 kg C y^{-1} during the peak upwelling season, each filament contributing to export of up to 22.6% of the organic carbon within the first 100 km from shore along the CanC EBUS (between 9.5 to 32 ° N). These results strongly support the inclusion of offshore transport estimates by coastal filaments in regional carbon budgets.

Keywords: biogeochemical modeling, upwelling filaments, Canary Current, ROMS, PISCES, organic carbon, offshore transport, eddy fluxes

1. Introduction

Upwelling filaments are ubiquitous mesoscale zonal features of the four main eastern boundary upwelling systems (EBUS) systems, i.e., the California, Humboldt, Canary and Benguela currents (Carr, 2001). Filaments are narrow ($\mathcal{O}$ (10 km)) elongated ($\mathcal{O}$ (100 km)) upper layer structures, typically 50-150 m deep, that contain relatively cool and fresh waters that originate from the eastern boundary coastal upwellings (Dewey et al., 1991; Lutjeharms et al., 1991; Haynes et al., 1993). They are usually identified by low-temperature (*Fig.* 1) and high-chlorophyll signals (Hagen et al., 1996), and are typically found close to coastal irregularities such as capes and headlands (Haynes et al., 1993). Filaments mediate exchange of water properties between eutrophic coastal upwelling systems and the adjacent oligotrophic open ocean (e.g., Álvarez-Salgado, 2007). Indeed, they have been observed to play a key role in transferring chlorophyll-a (chl-a; Álvarez-Salgado et al., 2001; Barth et al., 2002), organic matter (Fischer et al., 2000; García-Muñoz et al., 2005), and fish larvae (Brochier et al., 2011; Landeira et al., 2017) away from the richer near-shore upwelling to the open ocean. This transport may exceed Ekman transport (Álvarez-Salgado, 2007) and can extend the upwelling conditions several hundred kilometers offshore. In order to assess the impact of offshore transport by coastal filaments on regional carbon budgets, there is a need to better understand their variability and the mechanisms that drive them (Liu et al., 2000; Ducklow and McCallister, 2004).

The Canary Current (CanC) system supports several well known filaments at sites between Senegal and the Iberian peninsula (Van Camp et al., 1991). In particular, coastal filaments have been observed near Cape Blanc (∼20.0 ° N), Cape Juby (∼27.5 ° N), Cape Bojador (∼26.0 ° N) and Cape Ghir (∼30.5 ° N). The Cape Blanc giant filament (Karakaş et al., 2006) is intimately linked with the separation from the coast of the alongshore flow of the CanC (Mason et al., 2011) to join the North Equatorial Current (NEC; Stramma, 1984) in the region of the Cape Verde Frontal Zone (Pastor et al., 2008). Filaments at capes Juby and Bojador interact with mesoscale eddies associated with the Canary Islands (Arístegui et al., 2004; Sangrà et al., 2005). This system has been observed as either a single filament between Cape Juby and Cape Bojador (e.g., Arístegui et al., 1997;

Barton et al., 1998), or as two independent filaments, each attached at both capes, stemming from the coast and eventually merging offshore into a single structure (e.g., Pacheco and Hernandez-Guerra, 1999; Barton et al., 2000, 2004). Barton et al. (2004) described the system as having two filaments that detach from the coast south of Cape Juby and merge together offshore, with associated anticyclonic and cyclonic eddies that recirculate water back towards the shore. A major upwelling filament is also observed year round in the region of Cape Ghir, both in satellite images (e.g., Van Camp et al., 1991; Hernández-Guerra et al., 1993; Hernández-Guerra and Nykjaer, 1997), and from hydrographic cruises (e.g., Pelegrí et al., 1995, 2005b; Hagen et al., 1996; Antoranz et al., 1999). The origin of the Cape Ghir filament is thought to be caused by injection of cyclonic relative vorticity by strong surface wind stress curl over the coastal upwelling jet (Troupin et al., 2012; Sangrà et al., 2015).

Several studies (e.g., García-Muñoz et al., 2005; Santana-Falcón et al., 2016) have estimated that organic carbon export mediated by filaments in the subtropical northeast Atlantic might represent up to 63% of the annual primary production associated with the coastal upwelling. These estimates, however, could be biased if we assume that the instantaneous export transport is representative of the annual mean since the CanC system has high seasonal variability (Lathuilière et al., 2008; Cropper et al., 2014). Conventional methods that combine ship and satellite data are insufficient to provide synoptic three-dimensional views of filament dynamics since their coarse resolution precludes consideration of submesoscale variability. Therefore, although they have provided a first view of filament offshore transport, there is a need for finer scale studies that may reveal insights into their structure and effects on organic carbon distribution. Ocean models represent a powerful tool to understand the ocean carbon cycle (e.g., Aumont et al., 2003) that complement *in situ* and satellite observations with their higher time and space resolutions (e.g., Doney et al., 1996). However, despite their relevance, so far only the numerical study carried out by Lovecchio et al. (2018) has addressed the contribution of filament-mediated transport of organic carbon in this region.

In the present study, a climatological coupled physical-biogeochemical solution is used with the main objective of investigating the dynamics and variability of organic carbon transport within the filaments off Cape Ghir and Cape Juby (see *Fig.* 1). We provide here the first comprehensive study of the spatial and temporal variability of organic carbon transport mediated

by two coastal filaments in the Canary Current System.

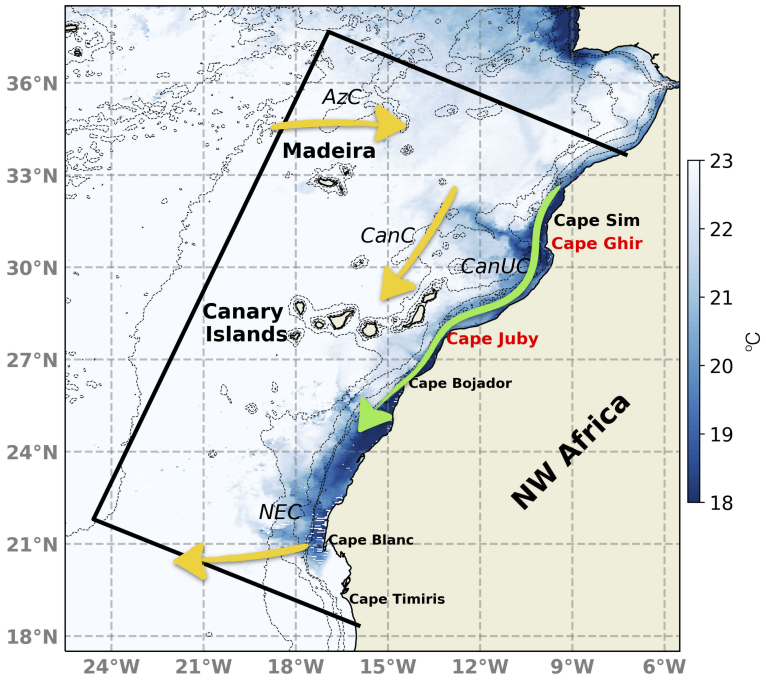

Figure 1: Schematic map of the Canary Basin showing the *CanBas4* domain (black line), major capes, the alongshore upwelling current (CanUC: Canary Upwelling Current; light green), and main currents (regular yellow). AzC: Azores Current; CanC: Canary Current; NEC: North Equatorial Current. 8-day composite of sea surface temperature from 21 to 28 of September 2016 is superimposed. Filaments off Cape Ghir (∼31 ° N) and Cape Juby (∼27.5 ° N) are identifiable by zonal cold tongues stretching offshore. Bathymetry from ETOPO is displayed (isobaths at 200, 1000, 2000, 3000, and 4000 m).

2. Material and methods

2.1. Hydrodynamic model and configuration

A monthly climatological simulation of the Regional Ocean Modeling System (ROMS; Shchepetkin and McWilliams, 2005, 2009) is conducted with a high-resolution three-dimensional configuration for the CanC. ROMS is a free surface primitive equation model that uses an orthogonal curvilinear coordinate system in the horizontal and a terrain-following (or sigma) coordinate in the vertical. It solves the barotropic and baroclinic momentum equations

separately. A non-local K-profile boundary layer scheme (KPP; Large et al., 1994) parameterizes unresolved subgrid-scale vertical mixing processes.

The model configuration has a horizontal resolution of 4 km, and 32 vertical sigma levels, with increased resolution over the mixed layer (between the surface and 120 m, stretching factors $\phi_s = 6$ and $\phi_b = 0$) where elevated biogeochemical activity is expected. Three open boundaries to the north, west and south permit inflow from a ROMS parent solution, with an update frequency at the boundaries of three days. The nesting procedure is one-way offline, so that only inflows from the ROMS parent affect the solution (Mason et al., 2010, *roms2roms*). The parent is the 50-year 7.5-km Canary Basin climatological solution of Mason et al. (2011). Initial conditions are interpolated from year 34 of this parent.

The 3D grid has 480 x 246 x 32 points, and covers the northwest African coastal upwelling (∼8-24°W, ∼17-37°N; ∼1750 km - 2200 km; see *Fig.* 1). The grid is rotated 28° clockwise to align with the African coast, thereby maximizing the number of sea-points on the grid.

The model is forced in climatological mode. Monthly mean climatological surface forcing leads to a statistically stationary seasonal cycle with intrinsic variability from year to year. Surface forcings come from the 1° Comprehensive Ocean-Atmosphere Data Set climatology (COADS; Worley et al., 2005) that provides heat and freshwater fluxes (precipitation), and the 0.25° monthly mean Scatterometer Climatology of Ocean Winds (SCOW; Risien and Chelton, 2008) based on eight years of QuikSCAT scatterometer wind data. Thermal forcing is linearized around the climatological sea surface temperature (SST; 9.28 km Pathfinder v.4) of Casey and Cornillon (1999).

Bathymetry data are taken from the 2′ resolution ETOPO2 topography (Smith and Sandwell, 1997). Models formulated with a terrain-following coordinate such as ROMS have computational restrictions with regards to the steepness and roughness of the topography (Beckmann and Haidvogel, 1993). Hence, a smoothing filter is applied to reduce the r-factor (Haidvogel and Beckmann, 1999). Following Mason et al. (2010) the topography near the boundaries of the nested domain is matched with the parent topography. Points where grid depths are shallower than 10 m are reset to 10 m.

2.2. Biogeochemical model

A biogeochemical model is coupled to the hydrodynamical configuration. We use PISCES (Pelagic Interaction Scheme for Carbon and Ecosystem Studies; Aumont and Bopp, 2006) to simulate marine biological productivity and

carbon biomass based upon the main nutrients: nitrate, ammonium, phosphate, silicate and iron. Biogeochemical boundary conditions are provided by monthly means from the World Ocean Atlas (WOA2009; Antonov et al., 2010). PISCES has been used in global simulations (e.g., Gehlen et al., 2006; Bopp et al., 2015), environmental studies (e.g., Rodgers et al., 2008; Brasseur et al., 2009), basin-scale studies (e.g., Gorgues et al., 2005; Jose et al., 2014) and, more recently, in regional scale studies (e.g., Resplandy et al., 2012; Echevin et al., 2014).

PISCES has 24 biogeochemical compartments. Among them, the model discretises three non-living compartments: the semi-labile dissolved organic carbon pool (DOC; Anderson and Williams, 1999), and two sizes of particulate organic carbon (POC) that differ by their sinking velocities (3 m d^{-1} for small particles, and 50 to 200 m d^{-1} for large particles). We refer to the inferred total organic carbon (TOC) throughout the text as excess TOC (e-TOC), i.e., the non-refractory pool of organic carbon, both dissolved and particulate. Particulate organic detritus is produced by mortality of nanophytoplankton and diatoms, fecal pellet production, grazing, and aggregation processes (e.g., Kriest and Evans, 2000). Excretion and mineralisation of POC, which is temperature dependent, account for the semi-labile pool of DOC. The ballast effect (e.g., Francois et al., 2002) is not accounted for in the model. A complete description of the PISCES formulation can be found in Aumont and Bopp (2006).

Since our objective is to study the variability of the organic carbon transport mediated by the coastal filaments at Cape Ghir and Cape Juby, we present results from seven years of the coupled solution (hereinafter *CanBas4*) after spin-up of one year. Throughout the text, negative (positive) values of across-shore organic carbon transport indicate offshore (onshore) fluxes. Note also that we use black rectangles as shown in *Fig.* 2 to indicate the two filament subdomains that will be referred to in the text and figures below.

3. CanBas4 validation

The ability of *CanBas4* to reproduce the dynamical and biogeochemical characteristics of the CanC system is presented. The physical model is assessed by comparing the simulated annual SST with annually averaged satellite SST observations from the Moderate Resolution Imaging Spectroradiometer (MODIS-Aqua; NASA 2014) sensor. An extended validation of the

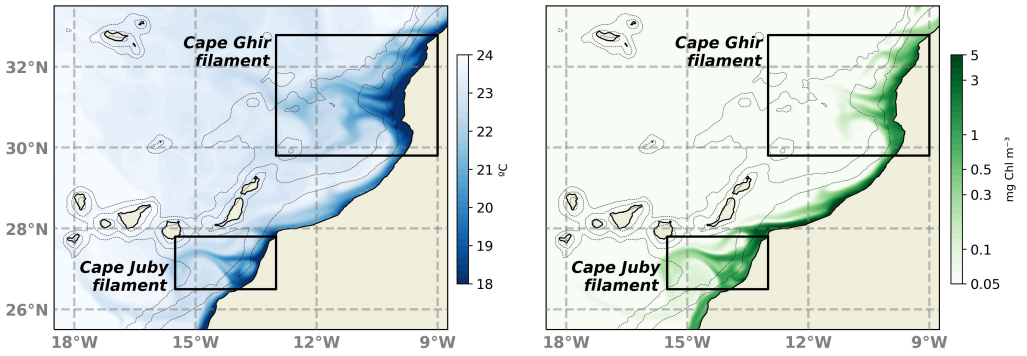

Figure 2: Snapshots of SST (left) and SChl (right) for a summer situation, 14 August, year 5, as simulated by *CanBas4*. Filament systems off Cape Ghir and Cape Juby are indicated by subdomains in black; the Cape Ghir subdomain spans from 9.0° to 13.0°W, 29.8° to 32.8°N. Cape Juby spans from 13.0° to 15.5°W, 26.5° to 27.8°N. The model bathymetry is displayed with gray contours (isobaths at 200, 1000, 2000, 3000 and 4000 m).

hydrodynamical parent solution is available in Mason et al. (2011).

A general evaluation of the phytoplankton biomass is carried out by comparing seasonal means of SChl with corresponding satellite means. In particular, modeled SChl is compared with 4-km resolution data from MODIS-Aqua accessible through `http://oceancolor.gsfc.nasa.gov/cgi/l3`.

The general distribution of SST in *CanBas4* shows a similar pattern to that of the satellite data (*Fig.* 3). However, as previously observed in other numerical studies in the region (e.g., Marchesiello and Estrade, 2009; Lachkar and Gruber, 2011; Auger et al., 2015), the model has a narrower cold upwelling band along the coast. This deviation is possibly related to a warm bias in the SST forcing dataset as observed by Dufois et al. (2012) in a number of modeling studies over the main EBUS where high SST gradients exist (e.g., Machu et al., 2009; Veitch et al., 2010; Albert et al., 2010; Echevin et al., 2011). The figure also shows the inability of *CanBas4* to reproduce the cool waters found in the inner shelf southward of ∼24 ° N. This bias may be attributed to uncertainties in the model nearshore wind structure (e.g., Veitch et al., 2010; Colas et al., 2012). The wind structure along coastal upwelling regions is not well constrained by surface wind products derived from scatterometers (Albert et al., 2010; Desbiolles et al., 2014), which poses a limitation when modeling these areas (e.g., Gruber et al., 2006).

Seasonal SChl maps in the area between 25.5° and 32.0 °N (*Fig.* 4) display

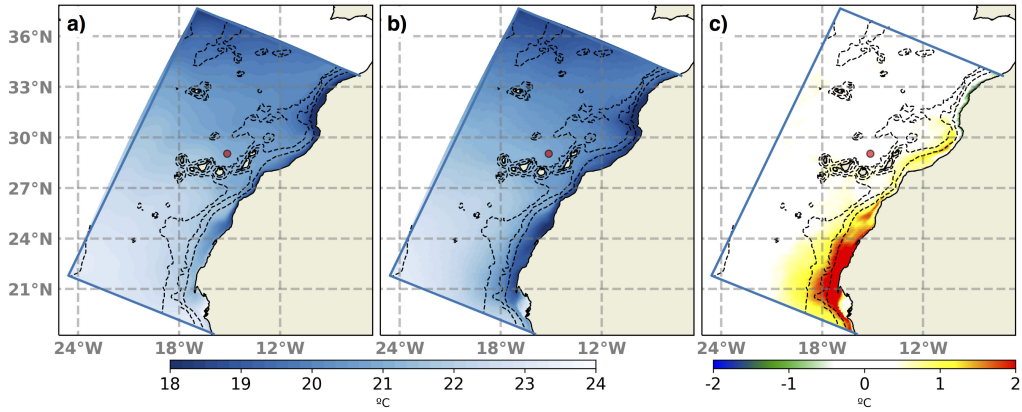

Figure 3: Annual means of (a) modeled SST (°C) averaged over seven years of the simulation compared with (b) 3-day averaged MODIS-Aqua climatology interpolated onto the model grid. (c) *CanBas4* minus MODIS-Aqua. Bathymetry lines from ETOPO are shown. Red dot indicates ESTOC site location.

the typical EBUS spatial patterns; concentrations are maximum nearshore (5-10 mg chl m^{-3}) as a consequence of the upwelling of nutrient-rich waters to the euphotic zone along the coast (Allen, 1973), and decrease gradually offshore towards the open ocean. Model means are consistent with satellite data in the offshore region, i.e., generally lower than 0.5 mg chl m^{-3}. Nearshore SChl values, however, are lower than satellite and, hence, the SChl gradient that defines the offshore limit of the coastal upwelling from the open ocean is not as sharp in the model. The characteristic seasonality of the region (e.g., Chavez and Messié, 2009; Cropper et al., 2014) due to both spatial and temporal variability in the wind stress forcing (Pradhan et al., 2006; Lathuilière et al., 2008) is well reproduced. During winter (January, February, and March; *Fig.* 4a, b), the absence of a seasonal thermocline due to convective mixing of the water column should be responsible for the highest SChl values year round in the open ocean, which barely exceed 0.3 mg chl m^{-3}. Nearshore SChl values are underestimated during this season. In spring (April, May, and June; *Fig.* 4c, d), the coastal upwelling is well reproduced. SChl extends further offshore at Cape Ghir and Cape Juby regions from this season to autumn, as also depicted in *Fig.* 3a of Lathuilière et al. (2008). The peak of plankton productivity occurs during summer (July, August, and September; *Fig.* 4e, f) when coastal upwelling is more intense (e.g., Lathuilière et al.,

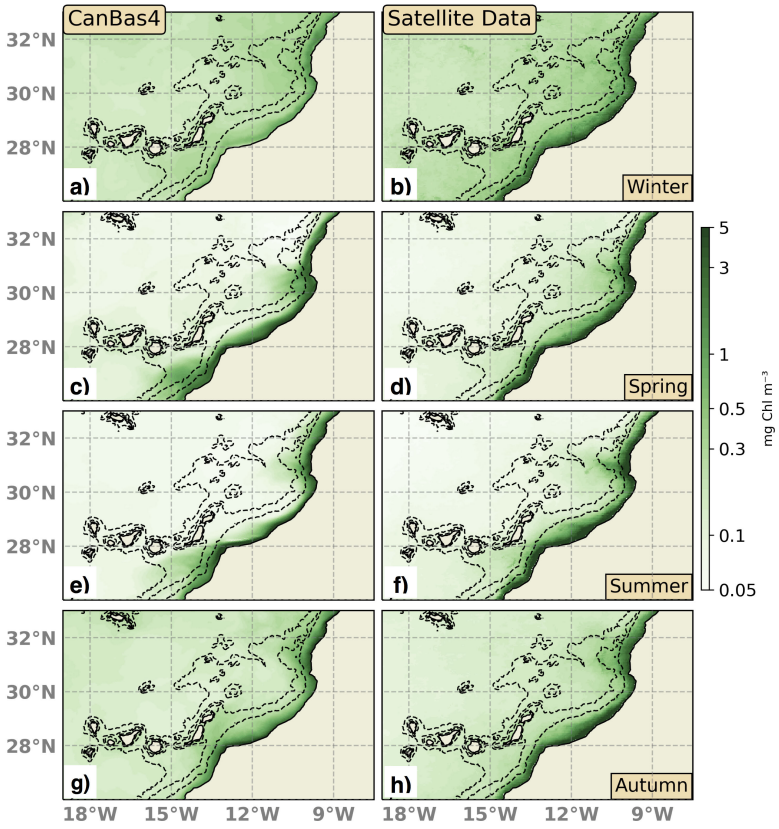

Figure 4: Seasonal means of model SChl over seven years of the simulation (left column; mg chl m^{-3}) compared with a 3-day average MODIS-Aqua climatology (right column; mg chl m^{-3}) for the central region (25.5° to 32.0°N) of the model grid. Winter corresponds to January, February, and March; Spring corresponds to April, May, and June; Summer corresponds to July, August, and September; Autumn corresponds to October, November, and December.

2008; Cropper et al., 2014). *CanBas4* reproduces this pattern qualitatively well; waters with negligible SChl dominate the open ocean region, while high values in the nearshore area create a strong cross-shore gradient. The most intense upwelling period lasts until autumn (e.g., Marcello et al., 2011) as evidenced by values higher than 5 mg chl m^{-3} near the coast and lower than 0.3 mg chl m^{-3} in the open ocean (October, November, and December; *Fig.* 4g, h). Additionally, the seasonality reproduced by *CanBas4* compares well with time-series data obtained from the ESTOC (European Station for Time

Series in the Ocean Canary Islands) site (red dot in *Fig.* 3; see Davenport et al., 1999; Neuer et al., 2007). In this open ocean area the highest values occur between January and March, and decrease until summer when surface values drop strongly to ∼0.05 mg chl m^{-3}.

4. Results

4.1. Upwelling and offshore transport

The long-term mean state of *CanBas4* provides context for the subsequent study of the transport driven by coastal filaments. Large alongshore variations of the annual mean horizontal flow averaged over the top 100 m of the water column are evident from a plan view presented in *Fig.* 5a. The satellite SST composite of *Fig.* 1 shows several tongues of cold upwelled waters stretching zonally over a few hundred kilometers at tne Cape Ghir (∼30.5 ° N) and Cape Juby (∼27.5 ° N) regions. SST and SChl snapshots from *CanBas4* displayed in *Fig.* 2 show the same pattern. The signals of these structures are smoothed out in the long-term means presented in *Fig.* 5, thus indicating that filaments must have significant variability in their latitudinal position.

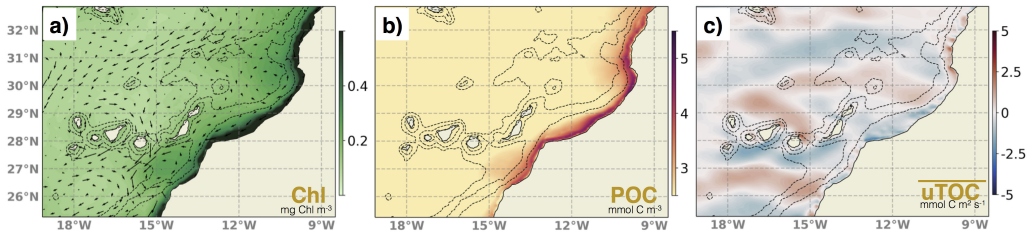

Figure 5: Plan view maps of annual mean quantities averaged over seven years of the simulation. (a) Chlorophyll averaged over the top 100 m (mg chl m^{-3}) with averaged horizontal velocity vectors superimposed (m s^{-1}); (b) POC averaged over the top 100 m (mmol C m^{-3}); (c) across-shore transport of e-TOC averaged over the top 100 m (mmol C m^{-2} s^{-1}). Negative (positive) values of across-shore e-TOC transport represent offshore (onshore) fluxes.

Maps of vertically averaged (0-100 m) chl-*a* and POC (*Fig.* 5 a, b) show that their concentrations are high near the coast but drop abruptly at the upwelling front. Values remain high, however, beyond the frontal region in both the Cape Ghir and Cape Juby regions. The depth-averaged distribution

of e-TOC (not shown) indicates a similar pattern at these points, but only in the first few meters of the water column (∼25-50 m). This is consistent with low DOC concentrations reported in the literature for recently upwelled waters (e.g., Álvarez-Salgado et al., 2001; García-Muñoz et al., 2005). The offshore transport of e-TOC ($\overline{uTOC}$) averaged over the top 100 m (*Fig.* 5c) shows a region of alternating intense offshore and weaker onshore standing meanders.

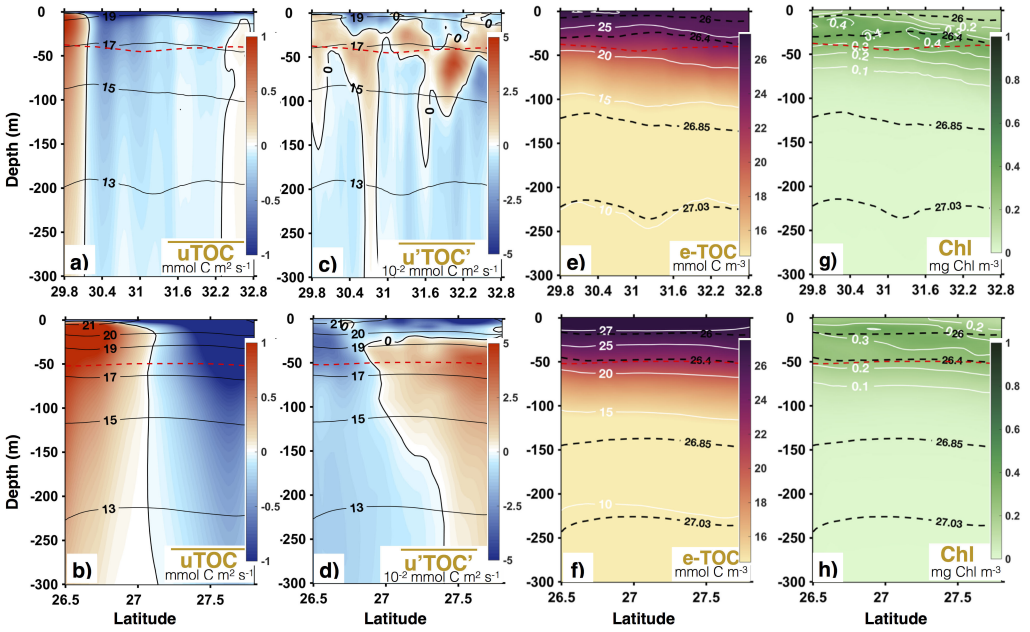

Figure 6: Long-term meridional mean sections at the Cape Ghir (10.6°W, 29.8° to 32.8°N; top panel) and Cape Juby (14.6°W, 26.5 to 27.8°N; bottom panel) filaments. The variables are (a, b) across-shore e-TOC transport ($\overline{uTOC}$; (mmol C m^{-2} s^{-1}), (c, d) across-shore eddy fluxes of e-TOC ($\overline{u'TOC'}$; 10 $^{-2}$ mmol C m^{-2} s^{-1}), (e, f) e-TOC (mmol C m^{-3}) with isotherms superimposed (°C), and (g, h) chl-*a* (mg chl m^{-3}) with isotherms superimposed (°C). Negative (positive) values of across-shore e-TOC transport represent offshore (onshore) fluxes. A contour indicating null across-shore e-TOC transport is added to plots a, b, c, and d. Neutral density layers are indicated by black dashed lines. Red dashed line indicates the mixed layer depth. X-axis represents latitude.

Meridional sections of the cross-shore annual mean situation at capes Ghir and Bojador indicate the existence of offshore fluxes at these coastal regions. However, the mean across-shore transport of e-TOC (i.e., $\overline{uTOC}$)

indicates some differences between the two cape regions (*Fig.* 6a, b). At Cape Ghir (upper panel), a strong negative flux, i.e., offshore transport, is seen centered at ∼30.4° N. Isolines of e-TOC and chl-*a* deepen on the northern side of this flux. A weak onshore flux below ∼15 m depth is found in the southern part of the section. Subsurface isopycnals create a concave shape between these two fluxes. By contrast, two large fluxes of opposing direction are evident in the Cape Juby section (lower panel). The offshore flux occupies the northernmost region of the section, being more intense at ∼27.6° N. Upper isolines of chl-*a* deepen at the northernmost part of this flux. The onshore flux is located below ∼15 m depth at the southern part of the section, just below the surface extension of the northern offshore flux. This positive flux is linked to a surface maximum of chl-*a* that extends to about 50 m depth.

4.2. Eddy fluxes

To investigate the components of the offshore fluxes previously observed in the annual mean figures, we compute eddy fluxes following the Reynolds decomposition method (e.g., Gruber et al., 2011; Nagai et al., 2015). We first calculated seasonal averages from the last seven years of *CanBas4*. We then subtract these means from the instantaneous values and the average to obtain the eddy fluxes. The eddy fluxes do not include processes with a time scale that is seasonal or longer, nor do they include processes with a time scale that is below the model output frequency (three days). Eddy fluxes of e-TOC are presented in meridional (*Fig.* 6c, d), and zonal (*Fig.* 7a, b) sections for both the Cape Ghir and Cape Juby regions.

Meridional sections of the annually averaged eddy-driven across-shore fluxes of e-TOC evidence the dominance of offshore fluxes across both cape regions (note that the color scales of the eddy flux figures are two orders of magnitude lower than long-term flux figures). Offshore eddy fluxes of carbon at Cape Ghir (*Fig.* 6c) occupy a large part of the section at the surface. A subsurface core (from 25 to 150 m) in which the eddy flux is positive crosses the section, being especially strong at about 32.0° N. At Cape Juby (*Fig.* 6d), an offshore eddy flux occupies the surface layer of the section, being stronger north of 27° N. This offshore flux deepens to 300 m in the southern part of the section. In the northern part of the section, a subsurface core (from 25 to 300 m) of positive transport is seen below the strong surface flux.

A zonal section of the across-shore e-TOC eddy flux at Cape Ghir (*Fig.* 7a) shows that mesoscale processes are active in the transport of organic

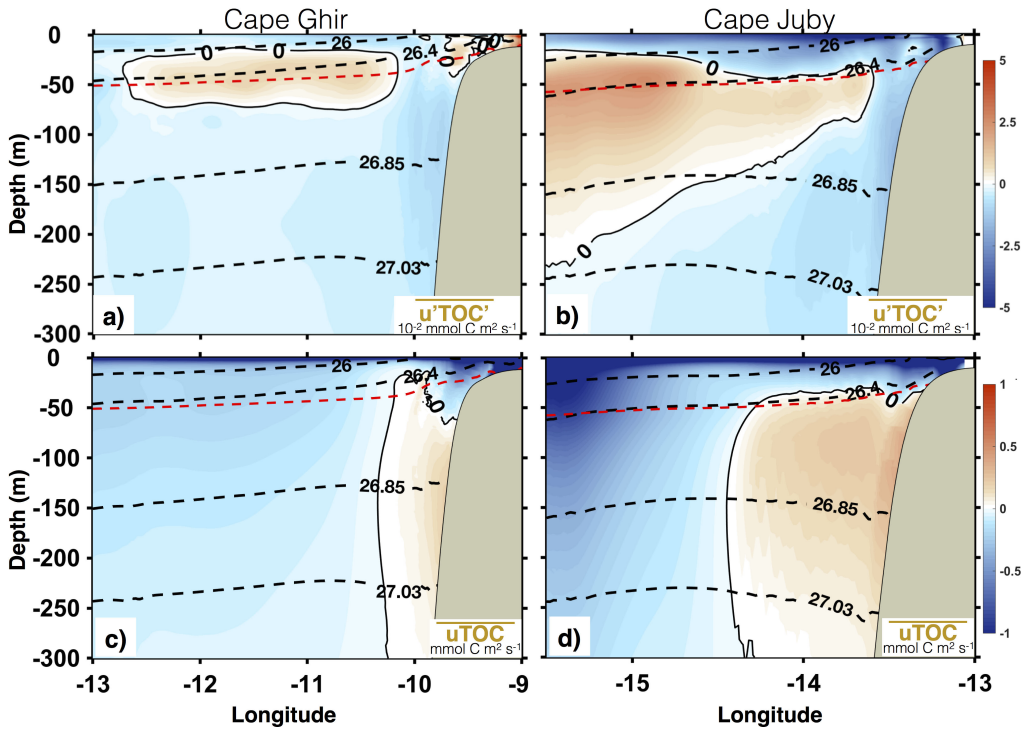

Figure 7: Meridionally averaged zonal sections of across-shore eddy (10^{-2} mmol C m^{-2} s^{-1}; upper panel) and mean (mmol C m^{-2} s^{-1}; lower panel) fluxes of e-TOC averaged over seven years of *CanBas4* at the Cape Ghir (a,c) and Cape Juby (b,d) filaments. See *Fig.* 2 for the capes Ghir and Juby domains. Negative (positive) values of across-shore e-TOC transport represent offshore (onshore) fluxes. Neutral density layers are indicated by black dashed lines. Red dashed line indicates the mixed layer depth. X-axis represents longitude.

matter away from the upwelling region. This offshore flux occurs preferentially at surface level along the whole section, but it also extends through the water column. The intensity of the transport reduces from the shore to the open ocean, but it is persistent more than 200 km offshore. An onshore transport core is seen at about 25-60 m depth extending offshore. Onshore transport is also observed in the first few meters of the water column at the coastal boundary.

The zonal section of the across-shore eddy flux of e-TOC at Cape Juby (*Fig.* 7b) shows that eddy currents act to transport organic matter from the upwelling region offshore. The intensity of the offshore transport is higher

than that observed at Cape Ghir, and occupies the first 50 m of the water column. This transport reduces as it deepens to subsurface waters of the continental slope and towards the offshore area. A positive flux below 50 m depth ($\sim$ the depth of the mixed layer depth) is seen relatively close to the shore. This onshore flux widens both upwards and downwards as it progresses offshore.

The across-shore mean fluxes of e-TOC are also presented in *Fig.* 7c, d for Cape Ghir and Cape Juby, respectively. The pattern of offshore transport of e-TOC seen at both filament regions is reproduced in these figures. The transport of organic carbon occurs preferentially in shallow waters and it extends several hundred kilometers offshore. In both filament systems, offshore transport dominates the first 300 m depth except for a positive onshore flux related to the coastal upwelling. Offshore fluxes seem to diminish and subduct as they progress offshore, indicating that organic carbon exported offshore may accumulate in subsurface waters.

4.3. Frontal structure of filaments

To investigate the structure of the filaments off Cape Ghir and Cape Juby, *Fig.* 8 and *Fig.* 9 show meridional sections (0-150 m) in both regions (subgrids in *Fig.* 2) for a summer situation (14 August of year 5) when their across-shore structures are visible. Though Cape Ghir and Cape Juby averages do not coincide with the annual average location shown in *Fig.* 6, they are selected in accordance with previous satellite and hydrographic observations (e.g., Hagen et al., 1996; Barton et al., 2004; Benítez-Barrios et al., 2011; Sangrà et al., 2015).

The coincidence of an upward tilt of isotherms in the near-surface layer above $\sim$50 m depth and a strong offshore transport of e-TOC (*Fig.* 8a) may indicate the position of the cold core of the filament off Cape Ghir (see Sangrà et al., 2015) at $\sim$31.4 °N. The doming of the isotherms extends into the water column (e.g., the 14°C isotherm) along with a relatively strong offshore flux that may correspond to the associated transport of the cool filament (see Sangrà et al., 2015), a broader and less intense structure. The snapshot shows a recirculating onshore jet south of $\sim$31.0 °N associated with warmer surface waters, while an intense offshore jet is observed north of it. In addition, north of $\sim$32.5 °N, a similar onshore jet that extends to deeper waters induces anticyclonic circulation, and is linked to the subduction of biogeochemical properties.

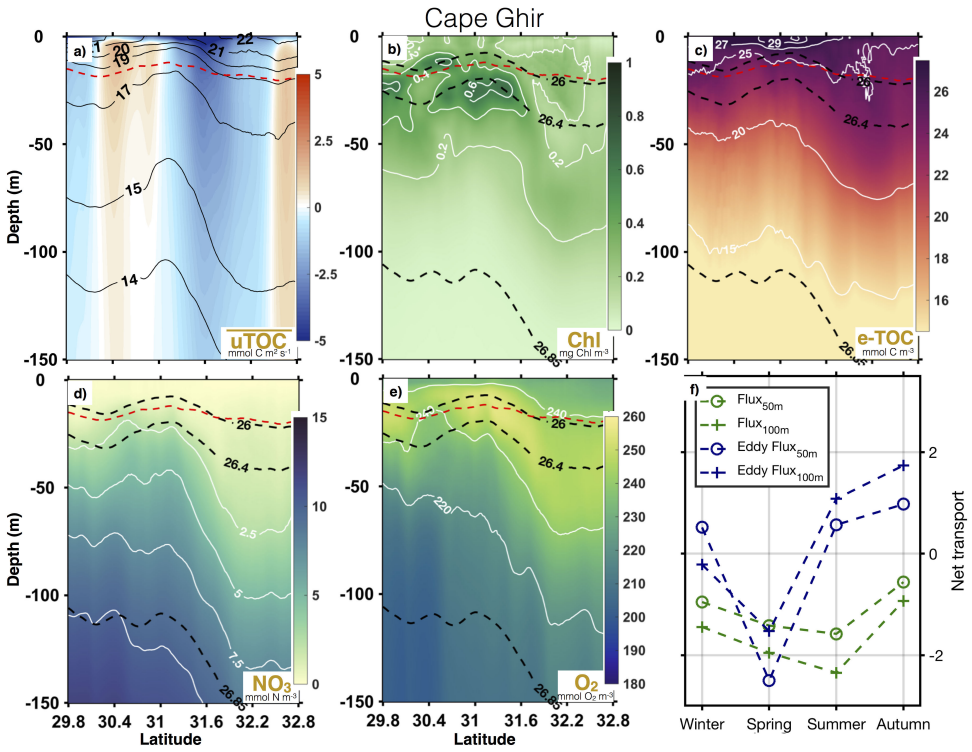

Figure 8: Meridional section averages at Cape Ghir (see *Fig.* 2 for the Cape Ghir domain) found in the simulation on 14 August year five for (a) across-shore e-TOC transport (mmol C m^{-2} s^{-1}) with isotherms superimposed (°C), (b) chl-*a* (mg Chl m^{-3}), (c) e-TOC (mmol C m^{-3}), (d) nitrate (mmol N m^{-3}), and (e) oxygen (mmol O_2 L^{-1}). (f) Seasonal net carbon mean (10^9 kg C y^{-1}) and eddy (10^7 kg C y^{-1}) fluxes across a meridional section at 10.6°W, 30.2° to 31.2°N. Negative (positive) values of across-shore e-TOC transport represent offshore (onshore) fluxes. Neutral density layers are indicated by black dashed lines. Red dashed line indicates the mixed layer depth.

The chl-*a* section (*Fig.* 8b) shows a subsurface (∼25 m) maximum associated with the cold filament that may result from the lateral advection of upwelled waters near the coast. Relatively high values are found at the cool filament front. Filaments are also rich in organic carbon (e.g., García-Muñoz et al., 2004, 2005; Santana-Falcón et al., 2016), but *CanBas4* has a more diffuse e-TOC distribution (see *Fig.* 8c) than that of temperature and chl-*a*. A surface e-TOC maximum is located in the core of the cold filament and extends above the southern onshore jet. e-TOC-rich waters are constrained

to the first ∼20-30 m of the water column creating a sharp vertical gradient, although sinking isolines north of the core indicate particle subduction. Even though nitrate is known to be rapidly exhausted within upwelling filaments, the nutrient-rich water upwelled off NW Africa (e.g., Barton et al., 1998) is also advected offshore within the near surface waters as evidenced by the relatively high nitrate concentration observed in the center of the dome (see *Fig.* 8d). The oxygen section (*Fig.* 8e) shows a surface relative maximum at the core that deepens northwards.

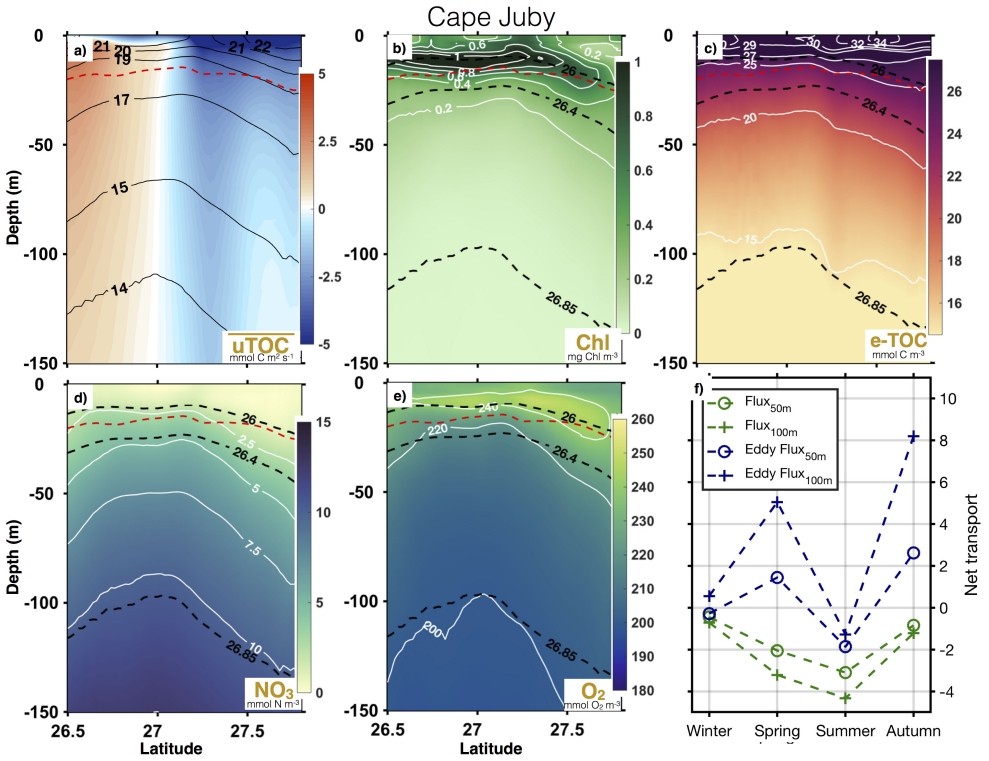

Figure 9: Meridional section averages at Cape Juby (see *Fig.* 2 for the Cape Juby domain) found in the simulation on 14 August year five for (a) across-shore e-TOC transport (mmol C m^{-2} s^{-1}) with isotherms superimposed (°C), (b) chl-*a* (mg Chl m^{-3}), (c) e-TOC (mmol C m^{-3}), (d) nitrate (mmol N m^{-3}), and (e) oxygen (mmol O_2 L^{-1}). (f) Seasonal net carbon mean (10^9 kg C y^{-1}) and eddy (10^7 kg C y^{-1}) fluxes across a meridional section at 14.6°W, 27.5 to 28.0°N. Negative (positive) values of across-shore e-TOC transport represent offshore (onshore) fluxes. Neutral density layers are indicated by black dashed lines. Red dashed line indicates the mixed layer depth.

The filament off Cape Juby is evident at ∼27.3° N where isotherms (and isopycnals) in the top ∼100 m shoal towards the surface as they move offshore. The offshore flow, stronger than observed at Cape Ghir, is located in the same area but extends to the north. A chl-*a* maximum between the surface and 25 m in *Fig.* 9b coincides with the position of the core. This chl-*a* maximum extends southward lying just above a strong onshore recirculation flux. A strong cyclonic circulation is, therefore, evident from these fluxes, in agreement with the filament generation mechanisms proposed by Barton et al. (2004) and Troupin et al. (2012). Additionally, a decrease of the offshore flux is seen in the subsurface waters (below ∼100 m) north of ∼27.5 °N.

e-TOC accumulates and is subducted by sinking isopycnals north of about 27.2°N (*Fig.* 9c). A sharp vertical gradient is created in the first 50 m of the water column at approximately 27.6°N, where relatively high values of chl-*a* are associated with slumping of isolines. As seen before, a local increase of nitrate concentration is found in the center of the isoneutrals dome (*Fig.* 9d). The oxygen section (*Fig.* 9e) has a surface relative maximum at the core that spreads both south and northward following the isoneutrals.

4.4. Seasonal carbon export

We estimated the seasonal mean and eddy fluxes of carbon (in kg C y^{-1}) across meridional sections in the regions off Cape Ghir (*Fig.* 8f) and Cape Juby (*Fig.* 9f). To compare with previous work, the sections coincide with those analysed by Santana-Falcón et al. (2016) at Cape Ghir (10.6°W, 30.2° to 31.2°N) and García-Muñoz et al. (2004) at Cape Juby (14.6°W, 27.5 to 28.0°N). The transport is estimated from surface to both 50 (circles) and 100 (crosses) m depth. Negative values represent offshore fluxes. Note that the eddy fluxes of carbon are 2 orders of magnitude lower than the mean fluxes.

The transport across both filaments is predominantly offshore during the annual cycle, and more intense in shallow waters. The net flux throughout the first 50 m of the water column represents more than 70% of the seasonal carbon net fluxes above 100 m. This is the result of both high e-TOC concentrations at this level and the intensity of the offshore-flowing jet. Additionally, the presence of recirculating onshore fluxes below 50 m diminishes the net transport of organic carbon towards the open ocean. Seasonal variability is evident in the net fluxes; the highest offshore fluxes over the annual cycle are recorded during spring and summer at both capes. Of particular

note is the relatively low transport obtained during autumn at both cape systems.

The net eddy fluxes of carbon throughout the sections offer a different view of that from the mean fluxes. The transport across the filament off Cape Ghir is onshore during the whole annual cycle, except during spring when offshore transport peaks. It is interesting to note that onshore fluxes are stronger in the first 50 m during winter. At Cape Juby the onshore transport peaks both in spring and autumn, but is predominantly offshore during summer.

5. Discussion

5.1. Net offshore transport

A rough estimate of the width of the cold nutrient-rich upwelling band is the Rossby radius of deformation (Allen, 1973) that ranges between 40-50 km in this particular region (Chelton et al., 1998). Vertical sections of model mean across-shore fluxes of e-TOC ($\overline{uTOC}$; see *Fig.* 6a,b) indicate, however, a strong offshore transport of cold upwelled waters stretching beyond this range. The mean offshore flow u (not shown) of up to 0.10 m s^{-1} is confined to the upper $\sim$25 m, consistent with previous observations (Pelegrí et al., 2005b) and model results (Troupin, 2011). Since the upwelling front tends to impede the Ekman-driven transport of material and properties into the open ocean (e.g., Brink et al., 1995), additional processes must be active in the region.

Our results from *CanBas4* demonstrate the role of upwelling filaments that stretch offshore (see *Fig.* 5), and highlight the important contribution of these structures to the lateral export of both organic carbon and chl-*a* from the upwelling region (see *Fig.* 8f and 9f). Across-shore carbon fluxes at both Cape Ghir and Cape Juby regions (*Fig.* 6 and *Fig.* 7) demonstrate that filament activity (that includes contributions from both eddy and mean fluxes of carbon) also contributes to the transport of organic carbon several hundreds of kilometers offshore year round. The pathways of the transport indicate that filaments preferentially export e-TOC near the surface. In addition, the vertical gradient of e-TOC concentrations observed at the frontal region of both capes (*Fig.* 6e, f) may indicate that these fluxes lead to the formation of a maximum of e-TOC below the surface (e.g., Arístegui et al., 2004).

Table 1: Comparison of inferred annual offshore transport of total organic carbon (e-TOC; 10^9 kg C y^{-1}) with estimates extracted from the literature for filaments in the NW Africa and northern Iberian upwelling regions.

Source	Region	Depth	Period	%DOC	Annual net transport
this study	Cape Ghir	100	simulation	90	0,9 to 2,3
	Cape Juby	100		90	0,7 to 4,3
Santana-Falcón et al., 2016	Cape Ghir	100	August 2009	70	2,1
García-Muñoz et al., 2005	Cape Ghir	100	September 1997	90	3,1
García-Muñoz et al., 2004	Cape Juby- Cape Bojador	100	August 1999	90	3,1
Álvarez-Salgado et al., 2001	Cape Finisterre	50	August 1998	50	0,4
Gabric et al., 1993	Cape Blanc	200	December 1983, March-October 1984	-	6,0

Several studies have already highlighted the role of filaments in enhancing offshore transport and downwelling of organic carbon in this region (e.g., Álvarez-Salgado, 2007; Fischer et al., 2009; Ohde et al., 2015). In a recent numerical study, Lovecchio et al. (2017) observed that lateral fluxes in the first 200 m below the surface are dominated by offshore fluxes in the northern region of the CanC, and these fluxes are strongly influenced by the presence of filaments. Nagai et al. (2015) showed evidence from a numerical study off California that filaments dominate the offshore transport and subduction of organic matter and nitrate within the first 200-300 km from the coast. However, despite their relative importance, the CanC Large Marine Ecosystem (Arístegui et al., 2009) is the only upwelling region where the net fluxes of e-TOC mediated by coastal filaments have been estimated so far. Average estimates of the annual net offshore transport of e-TOC extrapolated from those studies (Gabric et al., 1993; Álvarez-Salgado et al., 2001; García-Muñoz et al., 2004, 2005; Santana-Falcón et al., 2016) are compared with seasonal mean values obtained in the present simulation in *Table* 1.

Considering seasonal means, the inferred annual net transports mediated by the filaments off Cape Ghir, 0.9 to 2.3 $\times$ 10^9 kg C y^{-1}, and Cape Juby, 0.7 to 4.3 $\times$ 10^9 kg C y^{-1}, lie within the range of previous observational estimates. Gabric et al. (1993) estimated an annual export of $\sim$6 $\times$ 10^9 kg C y^{-1} for the region off Cape Blanc, suggesting this giant filament plays a central role in the export of carbon into the North Atlantic. Their estimates, however, could be dramatically underestimated since they were based solely on POC measurements and biomass estimation from satellite-based chl-a and, hence, do not account for the DOC contribution. Álvarez-Salgado et al. (2001) estimated an annual total export of 3.5 $\times$ 10^8 kg C y^{-1} for the filament off Cape Finisterre ($\sim$43 $^\circ$ N). The export associated with this Iberian filament is lower since it corresponds to a shallower feature ($\sim$50 m depth) that is active only during the summer upwelling season ($\sim$150 days;

Barton et al., 1998; Joint and Wassmann, 2001). García-Muñoz et al. (2005) and Santana-Falcón et al. (2016) studied the filament off Cape Ghir from a single oceanographic cruise carried out during weak and moderate upwelling conditions, respectively. Their estimates yield similar annual net transports of e-TOC (2.1 to 3.1 $\times$ 10^9 kg C y^{-1}). Santana-Falcón et al. (2016), however, showed more than three times higher POC export than García-Muñoz et al. (2005), suggesting that the POC/TOC ratio becomes higher as upwelling intensity increases. This argument agrees with the low POC/TOC ratio observed during the study of García-Muñoz et al. (2004), which was undertaken during upwelling-favorable but weak wind conditions. They observed two cold fresh-water filaments off Cape Juby that merged eventually some 100 km offshore (see Barton et al., 2004), and estimated a combined annual offshore transport of e-TOC of 3.1 $\times$ 10^9 kg C y^{-1}. In the present study, organic carbon is transported offshore mainly in the form of dissolved material in both filament systems. Since annual means in the simulation are the result of climatological averages and, hence, do not reflect synoptic conditions, it is plausible that POC contributions may be higher when upwelling activity increases and deviates from the mean state.

The average annual primary production for the upwelling waters of the CanC system has been estimated to range between 2 g C m^{-2} d^{-1} (Arístegui et al., 2006) and 3 g C m^{-2} d^{-1} (Carr and Kearns, 2003). Based on three net primary production models that made use of remote-sensing data, Gómez-Letona et al. (2017) has recently estimated an average primary production of 3 to 3.6 g C m^{-2} d^{-1} for the shelf region between 18.0 and 31.5 ° N. Assuming these averages, and taking into account that the region off Cape Ghir covers an area of about 6660 km^2, and the region off Cape Juby covers about 15000 km^2, the total primary production for the studied regions would range between 4.9 to 8.7 x 10^9 kg C y^{-1}, and between 10.9 to 19.7 x 10^9 kg C y^{-1}, respectively. If we consider the annual net transports of e-TOC estimated from *CanBas4*, the total primary production exported by the filaments off Cape Ghir and Cape Juby would represent, respectively, about 10.7 to 47.7%, and 3.5 to 39.6%, of the primary production associated with the upwelling. Furthermore, if we consider the net offshore flux of organic carbon estimated by Lovecchio et al. (2017) within the first 100 km from shore over the whole CanC EBUS (defined between 9.5 to 32 ° N) of 19 Tg C y^{-1}, each filament may contribute to the export of up to 22.6% of the organic carbon associated with the coastal upwelling. As a step further, Lovecchio et al. (2018) estimated that filament transport contributes 80% to the net offshore flux of

organic carbon. Considering this estimate, each filament may contribute up to 28.3% of this flux.

All the above observational studies were carried out during late summer and, therefore, their estimates can be considered as representative of the peak upwelling period. Filaments off the Iberian Peninsula are characterized by being active during the upwelling season (Haynes et al., 1993) but absent when the water flows north (Haynes and Barton, 1991; Barton et al., 1998). By contrast, filaments are known to be recurrent features in our region. A latitude/time plot (Hovmöller) of 3-day averages of temperature, chl-*a*, and e-TOC values from the model at 25 m depth off Cape Ghir (at 10.6° W) and Cape Juby (at 14.6° W) are shown in *Fig.* 10. Six annual cycles are plotted to better illustrate periodicity in the signals. The plots show a cold high-TOC and high-chl-*a* signal that appears every year in late spring - early summer in both regions. The growth of these signatures indicates seasonal variability in the zonal extension of the filaments. This behavior can also be observed in the seasonal offshore fluxes estimated here (see *Fig.* 8f and 9f). Plan views of e-TOC concentration averaged over the first 25 m of the water column with velocity vectors superimposed for both spring and autumn situations (*Fig.* 11) evidence the strong seasonal differences in the organic carbon dynamics.

The reduction of onshore recirculation loops during spring could be a consequence of two concomitant dynamic processes: the intensification of the southward flowing CanC, and the development of the equatorward coastal upwelling jet, the so-called CanUC (Canary Upwelling Current), north of Cape Ghir (see Pelegrí et al., 2006). The intensity of the CanC varies seasonally; it strengthens through spring and summer before moving offshore in fall (e.g., Mason et al., 2011; Pérez-Hernández et al., 2013). Meanwhile, the CanUC peaks in spring (Machín and Pelegrí, 2006) and flows along the coast during spring and summer, in concert with the seasonality of the prevailing winds (Pelegrí et al., 2005a; Cropper et al., 2014). The CanUC may reach velocities of up to 0.10 m s^{-1} (Machín et al., 2006). Accordingly, *Fig.* 11a shows waters with high e-TOC values that flow towards the open ocean in the Cape Ghir region, and southward following the upwelling jet. In the Cape Juby region, the signal of e-TOC transport away from the shore follows the same pattern, but it is lost in the high organic carbon content waters south of the Canaries (e.g., Arístegui et al., 1994, 1997; Barton et al., 1998).

Several studies (e.g., Machín and Pelegrí, 2009; Fraile-Nuez et al., 2010; Mason et al., 2011) have observed a northward flow in autumn at intermediate levels along the continental shelf between the African coast and the

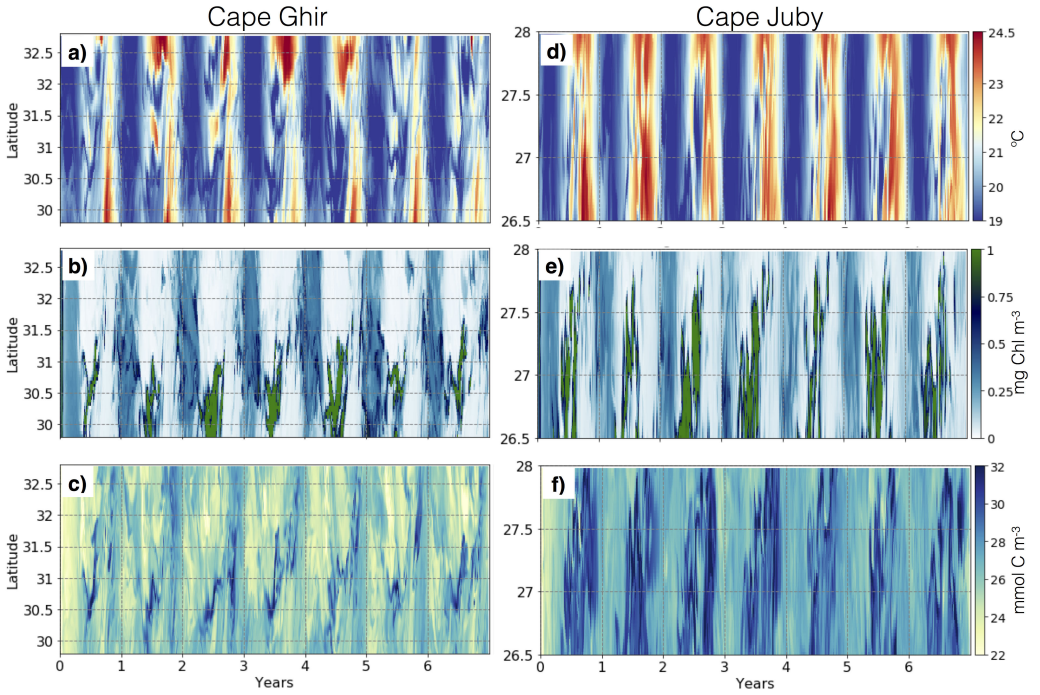

Figure 10: Latitude/time plots showing six repeated yearly cycles of 3-day averages of temperature (° C; top panel), chl-*a* (mg Chl m^{-3}; middle panel), and e-TOC (mmol C m^{-3}; lower panel) off Cape Ghir (at 10.6° W; left column) and Cape Juby (at 14.6° W; right column), at 25 m depth.

Canaries. This large scale flow (referred to as the Eastern Boundary Current in Fraile-Nuez et al., 2010; Mason et al., 2011) is equatorward at surface and central levels but reverses around November (Fraile-Nuez et al., 2010). *Fig.* 11b shows this poleward current may block the offshore flow of upwelling waters associated with the filament off Cape Juby, expanding the organic carbon signal northwards. In addition, Mason et al. (2011) observed that two anticyclonic / cyclonic anomalies develop north / south of the Cape Ghir region. These anomalies propagate offshore and thereby influence the position of the CanC. In autumn, the development of the anticyclonic anomaly could nudge the Cape Ghir filament northwards, thereby reducing its offshore transport through the section used in *Fig.* 8f. It could also transport substantial amounts of organic material into the open ocean, along with the separation from the coast of the CanC (Pelegrí et al., 2006). The map pre-

sented here shows that a fraction of the exported organic carbon enters this loop and extends some kilometers from the shore heading southwest. The net fluxes obtained in the present study indicate that the filament exports material offshore within the first 50 m of the water column. Below 50 m an eastward jet at the southern limit recirculates water and material onshore.

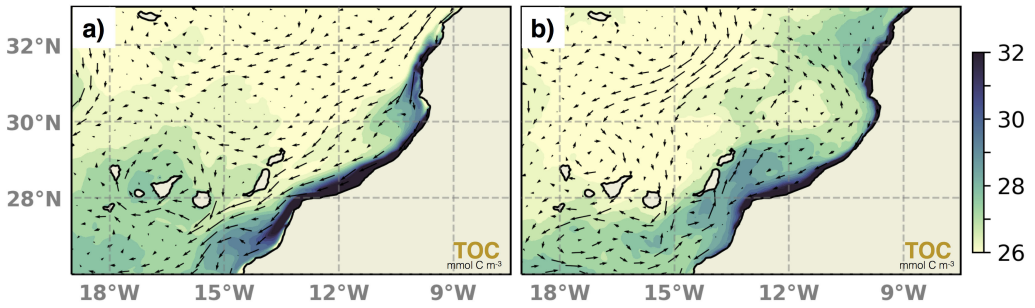

Figure 11: Plan view maps of e-TOC averaged over the top 25 m (mmol C m^{-3}) with averaged horizontal velocity vectors superimposed (m s^{-1}) for spring (a; left panel) and autumn (b; right panel) situations. Spring includes April, May, and June. Autumn includes October, November, and December.

In addition, we may also consider the relative contribution of eddy fluxes on the organic carbon transport mediated by filaments. Nagai et al. (2015) observed that eddy fluxes contribute to the transport of properties several hundreds of kilometers offshore. They observed this offshore transport occurs preferentially through the first 100 m depth. Likewise, Lovecchio et al. (2018) observed eddy fluxes of carbon to be predominantly offshore in the first 100 m depth in a major part of the CanC upwelling system. However, they observed onshore fluxes to be relevant in the region around Cape Ghir and Cape Juby. *Fig.* 6c, and 6d show offshore eddy fluxes dominate the transport in the upper waters across both cape systems. Nonetheless, in the Cape Ghir region, an onshore core following the bottom of the mixed layer (*Fig.* 7a) has a role in returning material towards the coast. The contribution of this flux to the annual net transport (see *Fig.* 8f) is, however, small to have a major effect. During spring, eddy fluxes of carbon reverse and their contribution coincide with the increasing of the net transport offshore.

Onshore eddy fluxes of carbon are more important in the Cape Juby region as illustrated in both zonal and meridional sections (*Fig.* 6d and 7b). According to our estimates, eddy fluxes contribute to the onshore transport

of organic carbon year round (see 9f). This juxtaposition with the dominantly offshore net transport of organic carbon may agree with Arístegui et al. (2004), who suggested that filament-eddy interactions are likely to govern the coastal-open ocean exchanges of organic carbon in this area. Particularly, offshore fluxes would depend on the interactions of the filament with a cyclonic eddy recurrently observed south of Fuerteventura (Barton et al., 2004; Benítez-Barrios et al., 2011). During autumn, onshore eddy fluxes of carbon are strong coinciding with the weakest offshore net transport in the annual cycle. This situation would agree with the low primary production rates measured in Arístegui and Montero (2005) during October. During summer, by contrast, eddy fluxes reverse and contribute to the peak of the offshore net transport of organic carbon.

5.2. Coastal filaments

The Cape Juby and Cape Ghir settings display differences that may arise due to both mesoscale activity and regional wind stress curl variability. As observed in the frontal structure off Cape Ghir (*Fig.* 8), the feature comprises a relatively cold tongue of shallow water with high chl-a and e-TOC concentrations that stretches zonally away from the shore. The narrowness of this structure may be maintained by strong eddy straining near the surface that creates sharp upwelling and downwelling fronts at both edges (McWilliams et al., 2009). This cold core is embedded within a larger 'cool' filament that extends the offshore transport to deeper waters in agreement with observations by Sangrà et al. (2015). Both filaments were bounded by northern offshore and southern onshore jets during the cruise carried out by Sangrà et al. (2015), and by two onshore flowing jets during the cruise carried out by García-Muñoz et al. (2005). In the simulation, an intense offshore-flowing cold tongue is located to the north, creating a cyclonic circulation pattern with a weaker southern tongue that transports oceanic waters onshore. In the northern region (north of about 32.4°N) an onshore jet that extends from 25 to 150 m depth is linked with the deepening of the isoneutrals. Pelegrí et al. (2005b) reported the recurrent signature of a subsurface anticyclonic mesoscale eddy-like structure consistent with an intrathermocline eddy (ITE; Hormazabal et al., 2013; Lee, 2018) that interrupts the offshore-flowing of the filament. Troupin (2011) observed a similar onshore jet at the northern edge of the filament characterized by warmer and saltier waters to be responsible for a downward velocity. Their numerical studies suggest it is a recurrent feature, and therefore it may have an impact on the regional carbon dy-

namics. Sangrà et al. (2015) observed no relationship between this structure and the poleward slope undercurrent as found in other studies (Cornuelle et al., 2000; Hormazabal et al., 2013), and suggested it may be linked to the secondary circulation of the filament. Further analysis would be necessary to confirm the nature of this structure in our simulation. Either way, a bowl-like structure is seen in the isolines of the properties displayed in the snapshot in *Fig.* 8 that is linked to anticyclonic circulation. This pattern of anticyclonic circulation at the northern front may be inferred from the annual mean across-shore fluxes of e-TOC (see *Fig.* 6a) by a weak onshore flux north of the offshore core. Moreover, the anticyclonic deflection of the SST in the northern region of the filament seen in *Fig.* 1 may also be indicative of this structure. From a biological point of view, the subduction of particles and properties associated with this anticyclonic structure may favor the prevalence of dissolved material in the surface layers of the filament, as indeed observed in previous *in situ* studies (García-Muñoz et al., 2005). This pattern of downwelling may highlight the role of the filament off Cape Ghir not only for export of carbon to the open ocean but also as a site for carbon subduction from the upper layers.

The position of the filament off Cape Juby is variable and depends on the intensity of the southward flowing CanUC and its interaction with the eddy field downstream of the Canaries. Interaction between the mesoscale eddies and filaments gives rise to strong horizontal gradients within a small geographical area (Barton et al., 2000), and favours exchange between the continental shelf and open ocean. *Fig.* 9 shows a strong onshore flow in the southern edge of the system, and an intense offshore flow in the northern edge where e-TOC accumulates and subducts following the isopycnals, as has been observed in anticyclonic eddies (e.g., Arístegui et al., 2003). The vertical transport in this region, associated with mesoscale activity downstream of the islands, promotes primary production and carbon export (e.g., Arístegui et al., 1997; Omand et al., 2015). In addition, a weak onshore jet seen below 100 m depth and just to the north of the frontal structure off Cape Juby could be related to the export of material to depth, as observed for the filament off Cape Ghir. In fact, Benítez-Barrios et al. (2011) observed that the mesoscale activity contribution to vertical motion at this anticyclonic eddy is the largest in the region.

5.3. Model limitations

The model solution has several limitations. (1) Ballasting of particles by their mineral composition (e.g., Ploug et al., 2008) is not specifically accounted for by PISCES and, thus, the model may underestimate sedimentation rates. Nonetheless, the settling velocity of particles parameterised here coincides with the range obtained by Alonso-González et al. (2010) using Indented Rotating Sphere Carousel (IRSC) sediment traps (Peterson et al., 2005) moored south of the Canaries. (2) The remineralisation of DOC is assumed to be constant below 120 m, and thus does not account for variability within the mesopelagic water layer where the major organic matter remineralization processes are thought to occur (Del Giorgio and Duarte, 2002). (3) The model does not include sediment resuspension, therefore impeding the formation of POC hotspots near the shelves (Alonso-González et al., 2009), and also limiting bottom transport over the slopes (Hwang et al., 2008). Since offshore transport below 200 m is generally small ($<$ 12% of total; Lovecchio et al., 2017) and filament structures do not extend to more than 100-150 m below the surface, we consider that the present simulation is able to determine and reproduce the lateral and vertical transports associated with filaments in the coastal upwelling region.

As shown in *section* 3, *CanBas4* is unable to reproduce the nearshore high SChl values observed by remotely-sensed data. These discrepancies give rise to the question of whether the model underestimates chl-*a* or, on the contrary, the satellite data overestimates it over the shelf. In this regard, the inferred chl-*a* lies within the range of *in situ* observations carried out in the region (e.g., Arístegui, 1990; Arístegui et al., 1997, 2003; Neuer et al., 2007). Furthermore, the inferred chl-*a* is also coherent with data collected annually along a meridional section north of the Canary Islands (RAPROCAN; Vélez-Belchí, P., unpublished data), and over the African shelf (COCA; Arístegui, J., unpublished data). The higher values from *CanBas4* in the region off Cape Juby during spring and summer in comparison with satellite products could be due to the high *CanBas4* spatial resolution. In addition, limitations of the climatological wind forcing to reproduce the total variance of the wind structure close to the shore (Marchesiello et al., 2003) is particularly critical when modeling upwelling areas (e.g., Gruber et al., 2006; Reboreda et al., 2014). The characteristic synoptic variability of this upwelling region (e.g., Arístegui et al., 2009; Cropper et al., 2014) may thus be poorly represented by our wind forcing dataset. Moreover, the warm bias along the coast observed in the annual SST comparison (see *Fig.* 3) will reduce the width and intensity

of the upwelling. This may imply that the retention of phytoplankton cells, nutrients, and organic carbon near the coast may equally be reduced by a weak cross-shore gradient between upwelled and non-upwelled waters, leading to a lower SChl signal (see *Fig.* 4). In addition, picophytoplankton ($< 2\ \mu$m), which is the most abundant size fraction for photosynthetic organisms in the Canary Island area (e.g., Montero, 1993) is not specifically diagnosed by the PISCES formulations.

The limited accuracy of satellite products, on the other hand, is a source of error; the presence of chromophoric dissolved organic matter, errors in the SChl algorithms in coastal regions (Le Fouest et al., 2006), and other imperfections could play a role in the discrepancies observed here. Several studies (e.g., Schollaert et al., 2003; Hyde et al., 2007) have shown remotely-sensed SChl to be overestimated in coastal regions because of increased concentrations of colored optical constituents in the water along with high concentrations of atmospheric aerosols. Gregg and Casey (2004) obtained a positive bias of $\sim$15% in the North Central Atlantic basin area and attributed this to proximity to Saharan dust plumes (Moulin et al., 2001).

6. Summary and conclusions

The role of coastal filaments in the export of organic carbon from the upwelling region of the CanC system is investigated using a coupled high-resolution ROMS-PISCES model forced by climatological fields. The relatively good agreement between the inferred physical and biogeochemical variables with real data allows us to estimate the seasonal and annual net offshore transports of organic carbon mediated by the filaments off Cape Ghir and Cape Juby with reasonable confidence, and to analyze the three-dimensional structure of both features. The results discussed here suggest that filament activity contributes significantly to the total lateral fluxes of organic carbon connecting the coastal upwelling region to the open ocean. Therefore, organic carbon transport mediated by filaments should be included in regional carbon budgets.

In general, e-TOC is advected within shallow waters some hundreds of kilometers offshore primarily driven by filaments detached from the coast. As the filament extends seaward it sinks creating a maximum of e-TOC that extends below the surface, consistent with previous observations (Barth et al., 2002; Arístegui et al., 2004; Bograd and Mantyla, 2005). The export peaks during late spring - early summer, driven by the intensification of the CanC

and CanUC systems. During autumn, however, the reversal of the eastern boundary current within a ∼100 km band off the African coast disturbs the zonal flows of both filament systems heading northwards, especially below 50 m depth. This seasonality stresses the need for observational studies of filaments at different periods of the year in order to make reliable estimates of their annual contributions to the net offshore transport of organic carbon.

The *CanBas4* solution has revealed the complex flow structure of both filaments. The filament off Cape Ghir comprises both onshore and offshore flows. In addition, an anticyclonic structure in the northern region may have an impact on organic carbon and property distributions since it is observed to be linked to downwelling of organic material. This subduction could increase POC export to depth (Omand et al., 2015), and could also reduce the overall amount of TOC exported towards the open ocean as suggested by Sangrà et al. (2015). By contrast, the filament off Cape Juby manifests itself as an intense offshore flow that injects high-chlorophyll and organic carbon waters into the numerous mesoscale eddies generated in the lee of the Canary Islands. This eddy field may have two important effects on the coastal-to-ocean exchange of organic carbon (Arístegui et al., 2004). On the one hand, the offshore transport of material to the open ocean initiated by the filament (Arístegui and Montero, 2005) may continue by the action of the westward propagating eddies. Sangrà et al. (2009) reported the region south of the Canary Islands to be an important source for long-lived westward moving eddies, which sometimes live for over six months while traveling more than 2000 km. As a result, the filament system and subsequent westward transport by mesoscale eddies could be an important source of organic carbon to the North Atlantic. On the other hand, these eddies may recirculate filament waters back to shore and hence reduce the filament's role in the exchange of organic carbon. To better understand how these mesoscale phenomena interact with the coastal filaments the next step is to extend our analyses to Lagrangian approaches (e.g., Mason et al., 2012; Chenillat et al., 2015b,a) that will allow us to track these dynamical pathways.

7. Acknowledgements

This research was supported by projects CAIBEX (CTM2007-66408-CO2-02) and FLUXES (CTM2015- 69392-C3-1-R) funded by the 'Spanish Plan

Nacional de I + D', and by projects SUMMER (AMD-817806-5) and TRIATLAS (AMD-817578-5) financed by the 'European Commission' to JA. EM acknowledges support from the Spanish Research Agency and the European Regional Development Fund (Award no. CTM2016-78607-P).

8. References

References

Aurélie Albert, Vincent Echevin, Marina Lévy, and Olivier Aumont. Impact of nearshore wind stress curl on coastal circulation and primary productivity in the Peru upwelling system. *Journal of Geophysical Research: Oceans*, 115(C12), 2010. doi: 10.1029/2010JC006569.

John S Allen. Upwelling and coastal jets in a continuously stratified ocean. *Journal of Physical Oceanography*, 3(3):245–257, 1973. doi: 10.1175/1520-0485(1973)003<0245:UACJIA>2.0.CO;2.

Iván J Alonso-González, Javier Arístegui, Juan Carlos Vilas, and Alonso Hernández-Guerra. Lateral POC transport and consumption in surface and deep waters of the Canary Current region: a box model study. *Global Biogeochemical Cycles*, 23(2), 2009. doi: 10.1029/2008GB003185.

Iván J Alonso-González, Javier Arístegui, Cindy Lee, Anna Sanchez-Vidal, Antoni Calafat, Joan Fabrés, Pablo Sangrá, Pere Masqué, Alonso Hernández-Guerra, and Verónica Benítez-Barrios. Role of slowly settling particles in the ocean carbon cycle. *Geophysical research letters*, 37(13), 2010. doi: 10.1029/2010GL043827.

Xosé Antón Álvarez-Salgado. Contribution of upwelling filaments to offshore carbon export in the subtropical Northeast Atlantic Ocean. *Limnology and Oceanography*, 52(3):1287–1292, 2007. doi: 10.4319/lo.2007.52.3.1287.

Xosé Antón Álvarez-Salgado, MD Doval, AV Borges, I Joint, M Frankignoulle, EMS Woodward, and FG Figueiras. Off-shelf fluxes of labile materials by an upwelling filament in the NW Iberian Upwelling System. *Progress In Oceanography*, 51, 2001. doi: /10.1016/S0079-6611(01)00073-8.

Thomas R Anderson and Peter J le B Williams. A one-dimensional model of dissolved organic carbon cycling in the water column incorporating combined biological-photochemical decomposition. *Global Biogeochemical Cycles*, 13(2):337–349, 1999. doi: 10.1029/1999GB900013.

JI Antonov, D Seidov, TP Boyer, RA Locarnini, AV Mishonov, HE Garcia, OK Baranova, MM Zweng, and DR Johnson. World Ocean Atlas 2009, vol. 2: Salinity, edited by: Levitus. *S., NOAA Atlas NESDIS*, 69:184, 2010.

AM Antoranz, A Ratsimandresy, JM Cortés, JL Pelegrı, A Hernández-Guerra, A Marrero-Dıaz, C Gordo, P Sangrá, A Rodrıguez-Santana, and A Martınez. Acoustic doppler current fields between the Strait of Gibraltar and the Canary Islands. In *CANIGO Conference, Las Palmas de Gran Canaria*, 1999.

J Arístegui, P Tett, A Hernández-Guerra, G Basterretxea, Ma F Montero, K Wild, P Sangrá, S Hernández-León, M Cantón, JA García-Braun, et al. The influence of island-generated eddies on chlorophyll distribution: a study of mesoscale variation around Gran Canaria. *Deep Sea Research Part I: Oceanographic Research Papers*, 44(1):71–96, 1997. doi: 10.1016/S0967-0637(96)00093-3.

Javier Arístegui. La distribución de la clorofila a en aguas de Canarias. 1990.

Javier Arístegui and María F Montero. Temporal and spatial changes in plankton respiration and biomass in the Canary Islands region: the effect of mesoscale variability. *Journal of Marine Systems*, 54(1):65–82, 2005. doi: 10.1016/j.jmarsys.2004.07.004.

Javier Arístegui, Pablo Sangrá, Santiago Hernández-León, M Cantón, Alonso Hernández-Guerra, and JL Kerling. Island-induced eddies in the Canary Islands. *Deep Sea Research Part I: Oceanographic Research Papers*, 41 (10):1509–1525, 1994. doi: 10.1016/0967-0637(94)90058-2.

Javier Arístegui, Eric D Barton, María F Montero, Mercedes García-Muñoz, and José Escánez. Organic carbon distribution and water column respiration in the NW Africa-Canaries Coastal Transition Zone. *Aquatic Microbial Ecology*, 33(3):289–301, 2003. doi: 10.3354/ame033289.

Javier Arístegui, Eric D Barton, Paul Tett, María F Montero, Mercedes García-Muñoz, Gotzon Basterretxea, Anne-Sophie Cussatlegras, Alicia

Ojeda, and Demetrio de Armas. Variability in plankton community structure, metabolism, and vertical carbon fluxes along an upwelling filament (Cape Juby, NW Africa). *Progress in Oceanography*, 62(2):95–113, 2004. doi: 10.1016/j.pocean.2004.07.004.

Javier Arístegui, Xose A Alvarez-Salgado, Eric D Barton, Francisco G Figueiras, Santiago Hernandez-León, Claude Roy, AMP Santos, AR Robinson, and K Brink. Oceanography and fisheries of the Canary Current/Iberian region of the Eastern North Atlantic. *The global coastal ocean: Interdisciplinary regional studies and syntheses*, 14:879, 2006.

Javier Arístegui, Eric D Barton, Xosé A Álvarez-Salgado, A Miguel P Santos, Francisco G Figueiras, Souad Kifani, Santiago Hernández-León, Evan Mason, Eric Machú, and Hervé Demarcq. Sub-regional ecosystem variability in the Canary Current upwelling. *Progress in Oceanography*, 83(1):33–48, 2009. doi: 10.1016/j.pocean.2009.07.031.

Pierre Amaël Auger, Eric Machu, Thomas Gorgues, Nicolas Grima, and Mathieu Waeles. Comparative study of potential transfer of natural and anthropogenic cadmium to plankton communities in the North-West African upwelling. *Science of the Total Environment*, 505:870–888, 2015. doi: 10.1016/j.scitotenv.2014.10.045.

Olivier Aumont and Laurent Bopp. Globalizing results from ocean in situ iron fertilization studies. *Global Biogeochemical Cycles*, 20(2), 2006. doi: 10.1029/2005GB002591.

Olivier Aumont, Ernst Maier-Reimer, Stéphane Blain, and P Monfray. An ecosystem model of the global ocean including Fe, Si, P colimitations. *Global Biogeochemical Cycles*, 17(2), 2003. doi: 10.1029/2001GB001745.

John A Barth, Timothy J Cowles, P Michael Kosro, R Kipp Shearman, Adriana Huyer, and Robert L Smith. Injection of carbon from the shelf to offshore beneath the euphotic zone in the California Current. *Journal of Geophysical Research: Oceans*, 107(C6), 2002. doi: 10.1029/2001JC000956.

ED Barton, J Arıstegui, P Tett, M Cantón, J Garcıa-Braun, S Hernández-León, L Nykjaer, C Almeida, J Almunia, S Ballesteros, et al. The transition zone of the Canary Current upwelling region. *Progress in Oceanography*, 41(4):455–504, 1998. doi: 10.1016/S0079-6611(98)00023-8.

Eric D Barton, Gotzon Basterretxea, Pierre Flament, E Gay Mitchelson-Jacob, Bethan Jones, Javier Arístegui, and Felix Herrera. Lee region of Gran Canaria. *Journal of Geophysical Research: Oceans*, 105(C7):17173–17193, 2000. doi: 10.1029/2000JC900010.

Eric D Barton, Javier Arístegui, Paul Tett, and Eleuteria Navarro-Pérez. Variability in the Canary Islands area of filament-eddy exchanges. *Progress in Oceanography*, 62(2):71–94, 2004. doi: 10.1016/j.pocean.2004.07.003.

Aike Beckmann and Dale B Haidvogel. Numerical simulation of flow around a tall isolated seamount. Part I: Problem formulation and model accuracy. *Journal of Physical Oceanography*, 23(8):1736–1753, 1993. doi: 10.1175/1520-0485(1993)023<1736:NSOFAA>2.0.CO;2.

Verónica María Benítez-Barrios, Josep Lluís Pelegrí, Alonso Hernández-Guerra, KMM Lwiza, Damià Gomis, Pedro Vélez-Belchí, and Santiago Hernández-León. Three-dimensional circulation in the NW Africa coastal transition zone. *Progress in Oceanography*, 91(4):516–533, 2011. doi: 10.1016/j.pocean.2011.07.022.

Steven J Bograd and Arnold W Mantyla. On the subduction of upwelled waters in the California Current. *Journal of Marine Research*, 63(5):863–885, 2005. doi: 10.1357/002224005774464229.

Laurent Bopp, Marina Lévy, Laure Resplandy, and Jean-Baptiste Sallée. Pathways of anthropogenic carbon subduction in the global ocean. *Geophysical Research Letters*, 42(15):6416–6423, 2015. doi: 10.1002/2015GL065073.

Pierre Brasseur, Nicolas Gruber, Rosa Barciela, Keith Brander, Maéva Doron, Abdelali Elmoussaoui, Alistair J Hobday, Martin Huret, Anne-Sophie Kremeur, Patrick Lehodey, et al. Integrating biogeochemistry and ecology into ocean data assimilation systems. *Oceanography*, 22(3):206–215, 2009.

KH Brink, FFG Abrantes, PA Bernal, RC Dugdale, M Estrada, L Hutchings, RA Jahnke, PJ Müller, and RL Smith. Group report: How do coastal upwelling systems operate as integrated physical, chemical, and biological systems and influence the geological record? The role of physical processes

in defining the spatial structures of biological and chemical variables. *Environmental Sciences Research Report ES*, 18:103–124, 1995.

Timothée Brochier, Evan Mason, Marta Moyano, Amina Berraho, Francois Colas, Pablo Sangrà, Santiago Hernández-León, Omar Ettahiri, and Christophe Lett. Ichthyoplankton transport from the African coast to the Canary islands. *Journal of Marine Systems*, 87(2):109–122, 2011. doi: 10.1016/j.jmarsys.2011.02.025.

Mary-Elena Carr. Estimation of potential productivity in Eastern Boundary Currents using remote sensing. *Deep Sea Research Part II: Topical Studies in Oceanography*, 49(1):59–80, 2001. doi: 10.1016/S0967-0645(01)00094-7.

Mary-Elena Carr and Edward J Kearns. Production regimes in four Eastern Boundary Current systems. *Deep Sea Research Part II: Topical Studies in Oceanography*, 50(22):3199–3221, 2003. doi: 10.1016/j.dsr2.2003.07.015.

Kenneth S Casey and Peter Cornillon. A comparison of satellite and in situ–based sea surface temperature climatologies. *Journal of Climate*, 12(6): 1848–1863, 1999.

Francisco P Chavez and Monique Messié. A comparison of eastern boundary upwelling ecosystems. *Progress in Oceanography*, 83(1):80–96, 2009.

Dudley B Chelton, Roland A Deszoeke, Michael G Schlax, Karim El Naggar, and Nicolas Siwertz. Geographical variability of the first baroclinic Rossby radius of deformation. *Journal of Physical Oceanography*, 28(3):433–460, 1998. doi: 10.1175/1520-0442(1999)012<1848:ACOSAI>2.0.CO;2.

Fanny Chenillat, Bruno Blanke, Nicolas Grima, Peter JS Franks, Xavier Capet, and Pascal Rivière. Quantifying tracer dynamics in moving fluids: a combined Eulerian-Lagrangian approach. *Frontiers in Environmental Science*, 3:43, 2015a. doi: 10.3389/fenvs.2015.00043.

Fanny Chenillat, Peter JS Franks, Pascal Rivière, Xavier Capet, Nicolas Grima, and Bruno Blanke. Plankton dynamics in a cyclonic eddy in the Southern California Current System. *Journal of Geophysical Research: Oceans*, 120(8):5566–5588, 2015b. doi: 10.1002/2015JC010826.

François Colas, James C McWilliams, Xavier Capet, and Jaison Kurian. Heat balance and eddies in the Peru-Chile current system. *Climate dynamics*, 39(1-2):509–529, 2012. doi: 10.1007/s00382-011-1170-6.

BD Cornuelle, TK Chereskin, PP Niiler, MY Morris, and DL Musgrave. Observations and modeling of a California undercurrent eddy. *Journal of Geophysical Research: Oceans*, 105(C1):1227–1243, 2000. doi: 10.1029/1999JC900284.

Thomas E Cropper, Edward Hanna, and Grant R Bigg. Spatial and temporal seasonal trends in coastal upwelling off Northwest Africa, 1981–2012. *Deep Sea Research Part I: Oceanographic Research Papers*, 86:94–111, 2014. doi: 10.1016/j.dsr.2014.01.007.

R Davenport, S Neuer, A Hernández-Guerra, MJ Rueda, O Llinas, G Fischer, and G Wefer. Seasonal and interannual pigment concentration in the Canary Islands region from CZCS data and comparison with observations from the ESTOC. *International Journal of Remote Sensing*, 20(7): 1419–1433, 1999.

Paul A Del Giorgio and Carlos M Duarte. Respiration in the open ocean. *Nature*, 420(6914):379–384, 2002.

Fabien Desbiolles, Bruno Blanke, Abderrahim Bentamy, and Nicolas Grima. Origin of fine-scale wind stress curl structures in the Benguela and Canary upwelling systems. *Journal of Geophysical Research: Oceans*, 119(11): 7931–7948, 2014.

Richard K Dewey, James N Moum, Clayton A Paulson, Douglas R Caldwell, and Stephen D Pierce. Structure and dynamics of a coastal filament. *Journal of Geophysical Research: Oceans*, 96(C8):14885–14907, 1991.

Scott C Doney, David M Glover, and Raymond G Najjar. A new coupled, one-dimensional biological-physical model for the upper ocean: Applications to the JGOFS Bermuda Atlantic Time-series Study (BATS) site. *Deep Sea Research Part II: Topical Studies in Oceanography*, 43(2):591–624, 1996.

Hugh W Ducklow and S Leigh McCallister. The biogeochemistry of carbon dioxide in the coastal oceans. *The sea*, 13:269–315, 2004.

François Dufois, Pierrick Penven, Christo Peter Whittle, and Jennifer Veitch. On the warm nearshore bias in Pathfinder monthly SST products over Eastern Boundary Upwelling Systems. *Ocean Modelling*, 47:113–118, 2012.

Vincent Echevin, Francois Colas, Alexis Chaigneau, and Pierrick Penven. Sensitivity of the Northern Humboldt Current System nearshore modeled circulation to initial and boundary conditions. *Journal of Geophysical Research: Oceans*, 116(C7), 2011.

Vincent Echevin, Aurélie Albert, Marina Lévy, Michelle Graco, Olivier Aumont, Alice Piétri, and Gilles Garric. Intraseasonal variability of nearshore productivity in the Northern Humboldt Current System: The role of coastal trapped waves. *Continental Shelf Research*, 73:14–30, 2014.

G Fischer, V Ratmeyer, and G Wefer. Organic carbon fluxes in the Atlantic and the Southern Ocean: relationship to primary production compiled from satellite radiometer data. *Deep Sea Research Part II: Topical Studies in Oceanography*, 47(9):1961–1997, 2000.

G Fischer, C Reuter, G Karakas, N Nowald, and G Wefer. Offshore advection of particles within the Cape Blanc filament, Mauritania: Results from observational and modelling studies. *Progress in Oceanography*, 83(1):322–330, 2009.

Eugenio Fraile-Nuez, Francisco Machín, Pedro Vélez-Belchí, Federico López-Laatzen, Rafael Borges, Verónica Benítez-Barrios, and Alonso Hernández-Guerra. Nine years of mass transport data in the eastern boundary of the North Atlantic Subtropical Gyre. *Journal of Geophysical Research: Oceans*, 115(C9), 2010.

Roger Francois, Susumu Honjo, Richard Krishfield, and Steve Manganini. Factors controlling the flux of organic carbon to the bathypelagic zone of the ocean. *Global Biogeochemical Cycles*, 16(4), 2002.

Albert J Gabric, Luis Garcia, Lieve Van Camp, Leo Nykjaer, Walter Eifler, and Wolfram Schrimpf. Offshore export of shelf production in the Cape Blanc (Mauritania) giant filament as derived from coastal zone color scanner imagery. *Journal of Geophysical Research: Oceans*, 98(C3):4697–4712, 1993.

Mercedes García-Muñoz, Javier Arístegui, María F Montero, and Eric D Barton. Distribution and transport of organic matter along a filament-eddy system in the Canaries–NW Africa coastal transition zone region. *Progress in Oceanography*, 62(2):115–129, 2004.

Mercedes García-Muñoz, Javier Arístegui, José L Pelegrí, Ana Antoranz, Alicia Ojeda, and Miriam Torres. Exchange of carbon by an upwelling filament off Cape Ghir (NW Africa). *Journal of Marine Systems*, 54(1): 83–95, 2005.

M Gehlen, L Bopp, N Emprin, Olivier Aumont, C Heinze, and O Ragueneau. Reconciling surface ocean productivity, export fluxes and sediment composition in a global biogeochemical ocean model. *Biogeosciences*, 3(4): 521–537, 2006.

Markel Gómez-Letona, Antonio G Ramos, Josep Coca, and Javier Arístegui. Trends in Primary Production in the Canary Current Upwelling System—A regional perspective comparing remote sensing models. *Frontiers in Marine Science*, 4:370, 2017.

Thomas Gorgues, C Menkes, Olivier Aumont, Jérôme Vialard, Yves Dandonneau, and Laurent Bopp. Biogeochemical impact of tropical instability waves in the equatorial Pacific. *Geophysical Research Letters*, 32(24), 2005.

Watson W Gregg and Nancy W Casey. Global and regional evaluation of the SeaWiFS chlorophyll data set. *Remote Sensing of Environment*, 93(4): 463–479, 2004.

Nicolas Gruber, Hartmut Frenzel, Scott C Doney, Patrick Marchesiello, James C McWilliams, John R Moisan, John J Oram, Gian-Kasper Plattner, and Keith D Stolzenbach. Eddy-resolving simulation of plankton ecosystem dynamics in the California Current System. *Deep Sea Research Part I: Oceanographic Research Papers*, 53(9):1483–1516, 2006.

Nicolas Gruber, Zouhair Lachkar, Hartmut Frenzel, Patrick Marchesiello, Matthias Münnich, James C McWilliams, Takeyoshi Nagai, and Gian-Kasper Plattner. Eddy-induced reduction of biological production in eastern boundary upwelling systems. *Nature geoscience*, 4(11):787–792, 2011.

E Hagen, C Zulicke, and R Feistel. Near-surface structures in the Cape Ghir filament off Morocco. *Oceanologica Acta*, 19(6):577–598, 1996.

Dale B Haidvogel and Aike Beckmann. *Numerical ocean circulation modeling*, volume 2. World Scientific, 1999.

R Haynes and Eric D Barton. Lagrangian observations in the Iberian coastal transition zone. *Journal of Geophysical Research: Oceans*, 96(C8):14731–14741, 1991.

R Haynes, Eric D Barton, and I Pilling. Development, persistence, and variability of upwelling filaments off the Atlantic coast of the Iberian Peninsula. *Journal of Geophysical Research: Oceans*, 98(C12):22681–22692, 1993.

A Hernández-Guerra and L Nykjaer. Sea surface temperature variability off north-west Africa: 1981-1989. *International Journal of Remote Sensing*, 18(12):2539–2558, 1997.

Alonso Hernández-Guerra, Javier Arístegui, Manuel Cantón, and Leo Nykjaer. Phytoplankton pigment patterns in the Canary Islands area as determined using Coastal Zone Colour Scanner data. *International Journal of Remote Sensing*, 14(7):1431–1437, 1993.

Samuel Hormazabal, Vincent Combes, Carmen E Morales, Marco A Correa-Ramirez, Emmanuel Di Lorenzo, and Sergio Nuñez. Intrathermocline eddies in the coastal transition zone off central Chile (31–41 S). *Journal of Geophysical Research: Oceans*, 118(10):4811–4821, 2013.

Jeomshik Hwang, Timothy I Eglinton, Richard A Krishfield, Steven J Manganini, and Susumu Honjo. Lateral organic carbon supply to the deep Canada Basin. *Geophysical Research Letters*, 35(11), 2008.

Peter Hyde, Ross Nelson, Dan Kimes, and Elissa Levine. Exploring LiDAR–RaDAR synergy predicting aboveground biomass in a southwestern ponderosa pine forest using LiDAR, SAR and InSAR. *Remote Sensing of Environment*, 106(1):28–38, 2007.

I Joint and P Wassmann. Lagrangian studies of the Iberian upwelling system—an introduction. A study of the temporal evolution of surface production and fate of organic matter during upwelling on and off the NW Spanish continental margin, 2001.

Yonss S Jose, Olivier Aumont, Eric Machu, Pierrick Penven, CL Moloney, and Olivier Maury. Influence of mesoscale eddies on biological production

in the Mozambique Channel: Several contrasted examples from a coupled ocean-biogeochemistry model. *Deep Sea Research Part II: Topical Studies in Oceanography*, 100:79–93, 2014.

G Karakaş, N Nowald, M Blaas, Patrick Marchesiello, Stephan Frickenhaus, and Reiner Schlitzer. High-resolution modeling of sediment erosion and particle transport across the northwest African shelf. *Journal of Geophysical Research: Oceans*, 111(C6), 2006.

Iris Kriest and Geoffrey T Evans. A vertically resolved model for phytoplankton aggregation. *Journal of Earth System Science*, 109(4):453–469, 2000.

Zouhair Lachkar and Nicolas Gruber. What controls biological production in coastal upwelling systems? Insights from a comparative modeling study. *Biogeosciences*, 8(10):2961, 2011.

José M Landeira, Timothée Brochier, Evan Mason, Fernando Lozano-Soldevilla, Santiago Hernández-León, and Eric D Barton. Transport pathways of decapod larvae under intense mesoscale activity in the Canary-African coastal transition zone: implications for population connectivity. *Scientia Marina*, 81(3):299–315, 2017.

William G Large, James C McWilliams, and Scott C Doney. Oceanic vertical mixing: A review and a model with a non local boundary layer parameterization. *Reviews of Geophysics*, 32(4):363–403, 1994.

Cyril Lathuilière, Vincent Echevin, and Marina Lévy. Seasonal and intraseasonal surface chlorophyll-a variability along the northwest African coast. *Journal of Geophysical Research: Oceans*, 113(C5), 2008.

V Le Fouest, Bruno Zakardjian, Francois J Saucier, and SA Cizmeli. Application of SeaWIFS-and AVHRR-derived data for mesoscale and regional validation of a 3-d high-resolution physical–biological model of the Gulf of St. Lawrence (Canada). *Journal of Marine Systems*, 60(1):30–50, 2006.

Dongkyu Lee. High concentration chlorophyll a rings associated with the formation of intrathermocline eddies. *Limnology and Oceanography*, 2018.

KK Liu, K Iseki, and SY Chao. Continental margin carbon fluxes. *The changing ocean carbon cycle*, pages 187–239, 2000.

Elisa Lovecchio, Nicolas Gruber, Matthias Münnich, and Zouhair Lachkar. On the long-range offshore transport of organic carbon from the Canary Upwelling System to the open North Atlantic. *Biogeosciences*, 14(13): 3337–3369, 2017.

Elisa Lovecchio, Nicolas Gruber, and Matthias Münnich. Mesoscale contribution to the long-range offshore transport of organic carbon from the canary upwelling system to the open north atlantic. *Biogeosciences*, 15 (16):5061–5091, 2018.

JRE Lutjeharms, FA Shillington, and CM Duncombe Rae. Observations of extreme upwelling filaments in the Southeast Atlantic Ocean. *Science*, 253 (5021):774, 1991.

Félix Machín, Alonso Hernández-Guerra, and Josep Lluís Pelegrí. Mass fluxes in the Canary Basin. *Progress in Oceanography*, 70(2):416–447, 2006.

Francisco Machín and Josep Lluís Pelegrí. Effect of the Canary Islands in the blockage and mixing of the North Atlantic eastern water masses. *Geophysical research letters*, 33(4), 2006.

Francisco Machín and Josep Lluís Pelegrí. Northward penetration of Antarctic intermediate water off Northwest Africa. *Journal of Physical Oceanography*, 39(3):512–535, 2009.

Eric Machu, O Ettahiri, S Kifani, A Benazzouz, A Makaoui, and Hervé Demarcq. Environmental control of the recruitment of sardines (sardina pilchardus) over the western saharan shelf between 1995 and 2002: a coupled physical/biogeochemical modelling experiment. *Fisheries Oceanography*, 18(5):287–300, 2009.

Javier Marcello, Alonso Hernandez-Guerra, Francisco Eugenio, and Abenauara Fonte. Seasonal and temporal study of the northwest African upwelling system. *International Journal of Remote Sensing*, 32(7):1843–1859, 2011.

Patrick Marchesiello and P Estrade. Eddy activity and mixing in upwelling systems: a comparative study of Northwest Africa and California regions. *International Journal of Earth Sciences*, 98(2):299–308, 2009.

Patrick Marchesiello, James C McWilliams, and Alexander Shchepetkin. Equilibrium structure and dynamics of the California Current System. *Journal of Physical Oceanography*, 33(4):753–783, 2003.

Evan Mason, Jeroen Molemaker, Alexander F Shchepetkin, Francois Colas, James C McWilliams, and Pablo Sangrà. Procedures for offline grid nesting in regional ocean models. *Ocean modelling*, 35(1):1–15, 2010.

Evan Mason, Francois Colas, Jeroen Molemaker, Alexander F Shchepetkin, Charles Troupin, James C McWilliams, and Pablo Sangrà. Seasonal variability of the Canary Current: A numerical study. *Journal of Geophysical Research: Oceans*, 116(C6), 2011.

Evan Mason, Francois Colas, and Josep Lluís Pelegrí. A Lagrangian study tracing water parcel origins in the Canary Upwelling System. *Scientia Marina*, 2012.

JC McWilliams, F Colas, and MJ Molemaker. Cold filamentary intensification and oceanic surface convergence lines. *Geophysical Research Letters*, 36(18), 2009.

MF Montero. *Respiración y actividad ETS en microplancton marino. Variabilidad del ETS en aguas de Canarias*. PhD thesis, PhD thesis. Universidad de Las Palmas de Gran Canaria, Spain, 1993.

Cyril Moulin, Howard R Gordon, Viva F Banzon, and Robert H Evans. Assessment of Saharan dust absorption in the visible from SeaWiFS imagery. *Journal of Geophysical Research: Atmospheres*, 106(D16):18239–18249, 2001.

Takeyoshi Nagai, Nicolas Gruber, Hartmut Frenzel, Zouhair Lachkar, James C McWilliams, and Gian-Kasper Plattner. Dominant role of eddies and filaments in the offshore transport of carbon and nutrients in the California Current System. *Journal of Geophysical Research: Oceans*, 120 (8):5318–5341, 2015.

Susanne Neuer, Andres Cianca, Peer Helmke, Tim Freudenthal, Robert Davenport, Helge Meggers, Michaela Knoll, J Magdalena Santana-Casiano, Melchor González-Davila, Maria-José Rueda, et al. Biogeochemistry and hydrography in the eastern subtropical North Atlantic gyre. Results from

the European time-series station ESTOC. *Progress in Oceanography*, 72 (1):1–29, 2007.

Thomas Ohde, Björn Fiedler, and Arne Körtzinger. Spatio-temporal distribution and transport of particulate matter in the eastern tropical North Atlantic observed by Argo floats. *Deep Sea Research Part I: Oceanographic Research Papers*, 102:26–42, 2015.

Melissa M Omand, Eric A D'Asaro, Craig M Lee, Mary Jane Perry, Nathan Briggs, Ivona Cetinić, and Amala Mahadevan. Eddy-driven subduction exports particulate organic carbon from the spring bloom. *Science*, 348 (6231):222–225, 2015.

Mercedes M Pacheco and Alonso Hernandez-Guerra. Seasonal variability of recurrent phytoplankton pigment patterns in the Canary Islands area. *International Journal of Remote Sensing*, 20(7):1405–1418, 1999.

Maria V Pastor, Josep L Pelegrí, Alonso Hernández-Guerra, Jordi Font, Jordi Salat, and Mikhail Emelianov. Water and nutrient fluxes off Northwest Africa. *Continental Shelf Research*, 28(7):915–936, 2008.

JL Pelegrí, A Antoranz, D Grisolía, A Hernández-Guerra, AW Ratsimandresy, and P Sangrà. Campaña Hespérides Octubre 1995, Cartagena-Las Palmas de Gran Canaria. *Unpublished internal report*, 1995.

JL Pelegrí, J Arístegui, L Cana, M González-Dávila, A Hernández-Guerra, S Hernández-León, A Marrero-Díaz, MF Montero, P Sangrà, and M Santana-Casiano. Coupling between the open ocean and the coastal upwelling region off northwest Africa: water recirculation and offshore pumping of organic matter. *Journal of Marine Systems*, 54(1):3–37, 2005a.

JL Pelegrí, A Marrero-Díaz, A Ratsimandresy, A Antoranz, J Cisneros-Aguirre, C Gordo, D Grisolía, A Hernández-Guerra, I Láiz, A Martínez, et al. Hydrographic cruises off northwest Africa: the Canary Current and the Cape Ghir region. *Journal of Marine Systems*, 54(1):39–63, 2005b.

Josep Lluís Pelegrí, A Marrero-Díaz, and AW Ratsimandresy. Nutrient irrigation of the North Atlantic. *Progress in Oceanography*, 70(2):366–406, 2006.

M Dolores Pérez-Hernández, Alonso Hernández-Guerra, Eugenio Fraile-Nuez, Isis Comas-Rodríguez, Verónica M Benítez-Barrios, J Francisco Domínguez-Yanes, Pedro Vélez-Belchí, and Demetrio De Armas. The source of the Canary current in fall 2009. *Journal of Geophysical Research: Oceans*, 118(6):2874–2891, 2013.

Michael L Peterson, Stuart G Wakeham, Cindy Lee, Meaghan A Askea, and Juan Carlos Miquel. Novel techniques for collection of sinking particles in the ocean and determining their settling rates. *Limnology and Oceanography: Methods*, 3(12):520–532, 2005.

Helle Ploug, Morten Iversen, and Gerhard Fischer. Ballast, sinking velocity and apparent diffusivity in marine snow and zooplankton fecal pellets: Implications for substrate turnover by attached bacteria. *Limnology and Oceanography*, 53:1878–1886, 2008.

Yaswant Pradhan, Samantha J Lavender, Nick J Hardman-Mountford, and James Aiken. Seasonal and inter-annual variability of chlorophyll-a concentration in the Mauritanian upwelling: Observation of an anomalous event during 1998–1999. *Deep Sea Research Part II: Topical Studies in Oceanography*, 53(14):1548–1559, 2006.

Rosa Reboreda, Rita Nolasco, Carmen G Castro, Xosé A Álvarez-Salgado, Nuno GF Cordeiro, Henrique Queiroga, and Jesus Dubert. Seasonal cycle of plankton production in the Iberian margin based on a high resolution ocean model. *Journal of Marine Systems*, 139:396–408, 2014.

Laure Resplandy, Marina Lévy, Laurent Bopp, Vincent Echevin, Stéphane Pous, VVSS Sarma, and MD Kumar. Controlling factors of the oxygen balance in the Arabian Sea's OMZ. 2012.

Craig M Risien and Dudley B Chelton. A global climatology of surface wind and wind stress fields from eight years of QuikSCAT scatterometer data. *Journal of Physical Oceanography*, 38(11):2379–2413, 2008.

Keith B Rodgers, Olivier Aumont, Christophe Menkes, and Thomas Gorgues. Decadal variations in equatorial Pacific ecosystems and ferrocline/pycnocline decoupling. *Global Biogeochemical Cycles*, 22(2), 2008.

Pablo Sangrà, Josep Lluís Pelegrí, Alonso Hernández-Guerra, Igor Arregui, JM Martín, A Marrero-Díaz, A Martínez, AW Ratsimandresy, and

A Rodríguez-Santana. Life history of an anticyclonic eddy. *Journal of Geophysical Research: Oceans*, 110(C3), 2005.

Pablo Sangrà, Ananda Pascual, Ángel Rodríguez-Santana, Francisco Machín, Evan Mason, James C McWilliams, Josep L Pelegrí, Changming Dong, Anna Rubio, Javier Arístegui, et al. The Canary Eddy Corridor: A major pathway for long-lived eddies in the subtropical North Atlantic. *Deep Sea Research Part I: Oceanographic Research Papers*, 56(12):2100–2114, 2009.

Pablo Sangrà, Charles Troupin, Beatriz Barreiro-González, Eric Desmond Barton, Abdellatif Orbi, and Javier Arístegui. The Cape Ghir filament system in August 2009 (NW Africa). *Journal of Geophysical Research: Oceans*, 120(6):4516–4533, 2015.

Yeray Santana-Falcón, Mar Benavides, Pablo Sangrà, Evan Mason, Eric Desmond Barton, Abdellatif Orbi, and Javier Arístegui. Coastal–offshore exchange of organic matter across the Cape Ghir filament (NW Africa) during moderate upwelling. *Journal of Marine Systems*, 154:233–242, 2016.

Stephanie E Schollaert, James A Yoder, John E O'Reilly, and Douglas L Westphal. Influence of dust and sulfate aerosols on ocean color spectra and chlorophyll a concentrations derived from SeaWiFS off the US east coast. *Journal of Geophysical Research: Oceans*, 108(C6), 2003.

Alexander F Shchepetkin and James C McWilliams. The regional oceanic modeling system (ROMS): a split-explicit, free-surface, topography-following-coordinate oceanic model. *Ocean Modelling*, 9(4):347–404, 2005.

Alexander F Shchepetkin and James C McWilliams. Correction and commentary for "Ocean forecasting in terrain-following coordinates: Formulation and skill assessment of the regional ocean modeling system" by Haidvogel et al., J. Comp. Phys. 227, pp. 3595–3624. *Journal of Computational Physics*, 228(24):8985–9000, 2009.

Walter HF Smith and David T Sandwell. Global sea floor topography from satellite altimetry and ship depth soundings. *Science*, 277(5334):1956–1962, 1997.

Lothar Stramma. Geostrophic transport in the warm water sphere of the eastern subtropical North Atlantic. *Journal of Marine Research*, 42(3): 537–558, 1984.

Charles Troupin. *Study of the Cape Ghir upwelling filament using variational data analysis and regional numerical model*. PhD thesis, University of Liege, Liege, Belgium, 2011.

Charles Troupin, Evan Mason, Jean-Marie Beckers, and Pablo Sangrà. Generation of the Cape Ghir upwelling filament: A numerical study. *Ocean Modelling*, 41:1–15, 2012.

L Van Camp, L Nykjaer, E Mittelstaedt, and P Schlittenhardt. Upwelling and boundary circulation off Northwest Africa as depicted by infrared and visible satellite observations. *Progress in Oceanography*, 26(4):357–402, 1991.

Jennifer Veitch, Pierrick Penven, and Frank Shillington. Modeling equilibrium dynamics of the Benguela Current System. *Journal of Physical Oceanography*, 40(9):1942–1964, 2010.

Steven J Worley, Scott D Woodruff, Richard W Reynolds, Sandra J Lubker, and Neal Lott. ICOADS release 2.1 data and products. *International Journal of Climatology*, 25(7):823–842, 2005.